IEEE Access
Multidisciplinary | Rapid Review | Open Access Journal

Received 2 December 2023, accepted 2 January 2024, date of publication 9 January 2024,
date of current version 19 January 2024.

Digital Object Identifier 10.1109/ACCESS.2024.3351809

RESEARCH ARTICLE

Unlocking the Potential of XAI for Improved Alzheimer's Disease Detection and Classification Using a ViT-GRU Model

S. M. MAHIM[1], MD. SHAHIN ALI[1], MD. OLID HASAN[1], ABDULLAH AL NOMAAN NAFI[2], AREFIN SADAT[3], SHAKIB AL HASAN[1], BRYAR SHAREEF[4], MD. MANJURUL AHSAN[5], MD. KHAIRUL ISLAM[1], MD. SIPON MIAH[2,6,7], (Senior Member, IEEE), AND MING-BO NIU[7], (Member, IEEE)

[1]Department of Biomedical Engineering, Islamic University, Kushtia 7003, Bangladesh
[2]Department of Information and Communication Technology, Islamic University, Kushtia 7003, Bangladesh
[3]Department of Medicine, Chandpur Medical College, Chandpur 3600, Bangladesh
[4]Department of Computer Science, University of Nevada, Las Vegas, Las Vegas, NV 89154, USA
[5]Machine and Hybrid Intelligence Laboratory, Department of Radiology, Northwestern University, Chicago, IL 60208, USA
[6]Department of Signal Theory and Communications, University Carlos III of Madrid (UC3M), Leganes, 28911 Madrid, Spain
[7]Internet of Vehicle[2] to Road Research Institute, Chang'an University, Xi'an, Shaanxi 710018, China

Corresponding author: Ming-Bo Niu (ivr.niu@chd.edu.cn)

This work was supported in part by the Islamic University funded by the Bangladesh Bureau of Educational Information and Statistics (BANBEIS), Ministry of Education, Government of the People's Republic of Bangladesh under Grant IC20201325; in part by the Ministry of Science and Technology of China under Grant G2021171024L; and in part by an Innovation Creative Centre Project of Shaanxi Province under Grant 300201000173.

ABSTRACT Alzheimer's Disease (AD) is a significant cause of dementia worldwide, and its progression from mild to severe affects an individual's ability to perform daily activities independently. The accurate and early diagnosis of AD is crucial for effective clinical intervention. However, interpreting AD from medical images can be challenging, even for experienced radiologists. Therefore, there is a need for an automatic diagnosis of AD, and researchers have investigated the potential of utilizing Artificial Intelligence (AI) techniques, particularly deep learning models, to address this challenge. This study proposes a framework that combines a Vision Transformer (ViT) and a Gated Recurrent Unit (GRU) to detect AD characteristics from Magnetic Resonance Imaging (MRI) images accurately and reliably. The ViT identifies crucial features from the input image, and the GRU establishes clear correlations between these features. The proposed model overcomes the class imbalance issue in the MRI image dataset and achieves superior accuracy and performance compared to existing methods. The model was trained on the Alzheimer's MRI Preprocessed Dataset obtained from Kaggle, achieving notable accuracies of 99.53% for 4-class and 99.69% for binary classification. It also demonstrated a high accuracy of 99.26% for 3-class on the AD Neuroimaging Initiative (ADNI) Baseline Database. These results were validated through a thorough 10-fold cross-validation process. Furthermore, Explainable AI (XAI) techniques were incorporated to make the model interpretable and explainable. This allows clinicians to understand the model's decision-making process and gain insights into the underlying factors driving the AD diagnosis.

INDEX TERMS Alzheimer's disease, deep learning, ViT-GRU, XAI, attention map.

I. INTRODUCTION

Alzheimer's Disease (AD) is by far the most prevalent trigger for dementia worldwide [1]. AD is a syndrome of progressive as well as irreversible dementia and is characterized by loss of cognitive abilities across multiple domains, changes in behavior, an inability to self-care, and ultimately neurological abnormalities [2]. A timely and effective diagnosis of AD is crucial for effective patient care and clinical progress [3]. It has been reported that AD affects around 5.8 million

The associate editor coordinating the review of this manuscript and approving it for publication was Hamed Azami.

individuals in the United States, representing 60-80% of all cases of dementia. It is anticipated that 13.8 million Americans will be afflicted with AD by the halfway point of this century. While AD commonly affects those aged 65 and above, the prevalence of early-onset cases indicates that it cannot be solely classified as a disease of old age [4]. Memory loss is the most common sign of AD [5]. There are typically three stages of AD: early, medium, and late. In the early stages of AD, individuals may experience mild cognitive and memory changes. They may have difficulty remembering recent events or conversations, struggle with problem-solving and decision-making, and undergo emotional and character shifts. They may also have difficulty completing familiar tasks. In the middle stage of AD, its symptoms become more prominent and significantly impact the person's daily life. They may become disoriented in familiar places or have difficulty following instructions. Communication may also become more difficult, with individuals struggling to find the right words or losing their train of thought mid-sentence. In the late stages of AD, individuals may experience a complete loss of ability to communicate effectively and become increasingly reliant on others for all aspects of their daily life. People with advanced AD are more likely to encounter infections, seizures, and other medical issues.

Researchers are looking at early detection of this condition to save medical expenditures and improve treatment outcomes, as well as to delay the atypical degeneration of the brain [6]. Positron Emission Tomography (PET) and Magnetic Resonance Imaging (MRI) are only two examples of cutting-edge brain imaging technologies that can be used to spot AD in its earliest stages. These techniques enable visualization of the brain's structure and function [7]. Metabolic shifts and protein aggregates like beta-amyloid and tau can be detected by PET imaging of the brain, which are hallmarks of AD. This imaging technique can identify changes in the brain even before disease symptoms appear. MRI imaging can produce anatomically accurate pictures of the brain and can be used to detect changes in brain volume, which may be indicative of AD. Diffusion Tensor Imaging (DTI) is an advanced MRI technique for assessing white matter tract integrity, which AD may impact. Cerebrospinal fluid and blood biomarker testing is another state-of-the-art technique that aids in the diagnosis of AD at its earliest stages. Researchers have identified several biomarkers in the blood and cerebrospinal fluid that are associated with AD, including beta-amyloid and tau proteins, as well as neuroinflammation markers. These biomarkers can be used to track disease progression and may help identify individuals at high risk for developing AD. Integrating available neuroimaging and biomarker testing for cerebrospinal fluid and blood can provide additional information, leading to a more precise and timely diagnosis of AD [8]. However, the current advanced diagnostic methods for AD are costly, invasive, and require a lot of time [9].

The utilization of Machine Learning (ML) in neuroimaging enhances the precision of diagnosing different types of dementia. To enable the implementation of ML algorithms, it is imperative to undertake specific pre-processing measures. These measures encompass the extraction and selection of features, reduction of feature dimensionality, and utilization of a classifier algorithm. Each of these phases plays a pivotal role in the classification process within ML [10].

To minimize human prejudice, later studies concentrated on employing Deep Learning (DL), an ML division that has demonstrated efficient usage in numerous healthcare fields.

This research adds to the growing evidence that MRI is the gold standard for analyzing brain structure because of its high spatial resolution, high tissue contrast, and restricted ionizing radiation [11]. It is critical to generate a reliable computer-aided diagnostic system that can examine MRI scans and identify AD. However, DL models can be time-consuming to address this issue. Our study proposes a hybrid DL model that combines a Vision Transformer (ViT) with a Gated Recurrent Unit (GRU), which outperforms existing Convolutional Neural Network (CNN) and ViT architectures in terms of both accuracy and time. The proposed model is designed to improve the accuracy of AD stage classification while minimizing computational costs by reducing the number of parameters.

This research comprises three distinct studies. The first and third studies entailed the execution of a multi-class classification, while the second study involved a binary classification task. Our research work has made several significant contributions, which are as follows:

1) We present a hybrid ViT-GRU approach that combines ViT and GRU to detect anomalies in brain MRI images. The model is capable of classifying AD from brain MRI images based on their structure and size.
2) A generalized model was developed and employed across three datasets, resulting in reduced parameters and computation costs. Despite these optimizations, the model exhibited exceptional performance in the diagnosis of AD.
3) We suggest the hybrid model that demonstrates the best performances in a shorter time frame compared to other CNN and ViT models.
4) We utilize three XAI techniques, namely Local Interpretable Model Agnostic Explanation (LIME), Shapley Additive Explanations (SHAP), and Attention map to provide clear and interpretable explanations for the predictions generated by our ViT-GRU model. It enables us to validate the significance of specific features, compare and contrast the results obtained from various methods, and emphasize the clinical relevance of our model.
5) Our findings reveal that, despite the class imbalance in the dataset, our model's performance was remarkably high due to effective feature engineering and modeling

strategies, which could have significant implications for improving ML applications and facilitating its adoption in the clinical domain.

This remaining paper is organized as follows: Section II presents a comprehensive analysis of the current literature on the classification of AD. Section III discusses the challenges associated with the application of AI for detecting neurodegenerative diseases. The materials and methods utilized in this study are described in detail in Section IV. Section V presents the analysis of the results, while Section VI discusses the findings. Finally, Section VII concludes the paper.

II. LITERATURE REVIEW

Identifying AD at its incipient stage and with better accuracy is significant for improving the quality of life for patients and potentially slowing or halting the progression of the disease [12]. The potential of DL in human disease identification has garnered a lot of interest. Over the past few years, there has been a surge in the development of DL techniques for diagnosing AD, which have become popular diagnostic tools for medical professionals. These DL approaches are favored above more conventional types of ML [13].

Basheer et al. [14] introduced a CNN model called CapNet, which achieved an accuracy of 92.39% on the Open Access Series of Imaging Studies (OASIS) dataset. Meanwhile, Liu et al. [15] introduced a DL model comprising stacked auto-encoders and a softmax output layer to improve the diagnosis of Mild Cognitive Impairment (MCI) and AD. The goal was to address the bottleneck issue and aid in the early detection of these conditions. Their model produced an overall accuracy of 87.76% in the two-class classification of AD. Ortiz et al. [16] introduced a technique utilizing an ensemble CNN model and Softmax classifier to diagnose AD. The AD neuroimaging initiative provided the data used to validate the model. The model architecture performed exceptionally well, with an accuracy of 90% or higher for Normal Control (NC)/AD classification and an Area Under Curve (AUC) of 95%. It also performed well for stable MCI/AD classification with an accuracy of 84% and an AUC of 91% and for NC/MCI converter classification with an accuracy of 83% and an AUC of 95% [17]. On the other hand, Nawaz et al. [18] devised a way to classify AD stages by utilizing a pre-trained Alexnet model as a feature extractor to address class imbalance issues. The classification was done using Support Vector Machine (SVM), K-Nearest Neighbors (KNN), and Random Forest (RF) algorithms, resulting in a maximum accuracy of 99.21%. Basaia et al. [19] introduced a deep neural network method for diagnosing AD using the ADNI dataset. The study divided 1638 subjects into four categories, and the experiment used a 90% training and 10% testing ratio. The method achieved a 99.20% classification rate for distinguishing between healthy individuals and those with AD. In contrast, Sun et al. [20] employed a DL model named ResNet that could detect early-stage AD, including Spatial Transformer Networks (STN) and non-local attention mechanisms.

With a 97.10% classification rate, 95.50% macro precision, 95.30% macro recall, and 95.4% macro F1-score, the algorithm performed quite well. For feature extraction, Jain et al. [21] employed a pre-trained VGG16 model, and for MRI pre-processing, they turned to the FreeSurfer technique. They selected slices using entropy and applied transfer learning with a mathematical model called PF SECTL for the AD classification. The ADNI dataset was used to classify NC, early MCI (EMCI), and late MCI (LMCI), with an accuracy of 95.73% achieved. Independent component analysis was introduced by Schouten et al. [22] to examine diffusion MRI data from 77 AD patients and 173 controls. With an area under the curve of 89.60%, their research showed excellent promise for diagnosing AD. For the purpose of learning AD-related features, Ge et al. [23] developed a Three-dimensional (3D) multiscale DL model employing a dataset of brain scans from several participants randomly split into subsets. The model was found to be accurate on average to the tune of 87.24% and in testing to the tune of 93.53%. In order to make an accurate diagnosis of AD, Feng et al. [24] introduced a new DL architecture that combines 3D-CNN with Fully Stacked Bidirectional Long Short Term Memory (FSBi-LSTM). The study determined that the proposed method achieved mean accuracies of 94.82%, 86.36%, and 65.35% on the ADNI dataset, respectively, when tasked with differentiating between AD and NC, prodromal MCI (pMCI), and stable MCI (sMCI). While the study's findings show promise for the suggested paradigm, a thorough and efficient diagnosis of AD will require substantial computational resources. Allioui et al. [25] introduced a deep U-Net network for MRI segmentation. They demonstrated competitive results in detecting damaged brain Regions of Interest (ROIs) and diagnosing AD. They achieved an accuracy of 92.71%, a sensitivity of 94.43%, and a specificity of 91.59% on the OASIS dataset. Balasundaram et al. [26] introduced a DL-based approach in which they trained a Kaggle dataset for severity classification. Additionally, they conducted segmentation of the hippocampus region using a reduced version of the OASIS dataset and trained it using supervised and ensemble learning algorithms to detect AD. They achieved an accuracy of 94.45% for the Kaggle dataset and 94% for the OASIS dataset.

Previous studies on AD diagnosis using DL models faced challenges like limited accuracy, class imbalance, high computational demands, limited interpretability, and constrained generalizability. However, our proposed ViT-GRU model effectively addresses these limitations and presents improvements in multiple aspects. While previous DL models achieved notable accuracy in AD classification, our ViT-GRU model surpasses their performance, exhibiting exceptional accuracy and showcasing superior capability [27], [28]. Class imbalance within datasets has been a challenge for AD classification. Previous approaches used pre-trained models and feature extraction methods to handle this

issue [29]. Similarly, our model, employing ViT and GRU layers, effectively tackles class imbalance and enhances classification accuracy [30]. Efficient AD diagnosis requires significant computational resources, which can be limited in clinical settings. Our ViT-GRU model aims to provide comprehensive and efficient AD diagnosis while considering the practicality of clinical environments and optimizing computational resources if necessary. Interpretability of DL models has been a limitation, hindering understanding of the decision-making process behind predictions. Our model incorporates XAI techniques such as LIME, SHAP, and Attention map, providing valuable insights into the features and regions influencing its predictions, enhancing interpretability, and establishing trust. Previous studies often focused on specific datasets or cohorts, limiting model generalizability. Utilizing a ViT-GRU architecture enables the capture of spatial and temporal information from diverse datasets, enhancing the model's ability to generalize across different populations and imaging protocols and expanding its applicability to a wider range of scenarios.

III. CHALLENGES OF NEURO DISEASE DETECTION WITH AI

The healthcare sector has numerous challenges that prevent companies from increasing the efficiency and quality of patient treatment despite rising prices and demand. Several cutting-edge approaches to neurological care have shown positive results and present exciting new areas for investigating assessment, therapy planning, and prognosis prediction. There are not enough medical personnel or equipment to fulfill the rising demand. AI and other digital and technology solutions are now a real alternative for dealing with some of the problems in healthcare [31], [32], [33]. AI-supported technologies are crucial for enhancing the decision-making process used when treating and diagnosing patients since they make it easier for doctors to learn from and assess a vast amount of medical research and patient treatment records [34], [35]. Although this technology will eventually have a significant effect on the clinic practice patterns, translating it into clinical practice is difficult and requires the same levels of transparency and efficacy as any novel drug or medical device due to the possibility of bias and ethical, medical, and legal issues. Challenges associated with the detection of neurodiseases using AI are listed below:

1) **Limited data availability:** To learn, AI algorithms require vast quantities of high-quality data. Nevertheless, acquiring large datasets of neurological disease patients can be challenging due to privacy concerns, limited access to patient data, and the low incidence of certain neurodiseases [36].
2) **Heterogeneity of data:** Neurological pathologies can manifest in various ways and affect various brain regions, resulting in a vast array of symptoms and imaging characteristics. This diversity makes it difficult to develop AI models that accurately identify and categorize various neurodegenerative diseases [37].
3) **Lack of standardization in imaging protocols:** Different methods of imaging (such as Computed Tomography (CT), MRI, and PET) can generate distinct types of images, and institution-specific imaging protocols are frequently variable [38].
4) **Interpretability of AI models:** Models based on DL can be extremely complex and challenging to interpret, rendering it difficult to comprehend how the model makes predictions [39].
5) **Ethical considerations:** Implementing AI for detecting neurological diseases addresses major ethical considerations such as patient privacy, informed consent, and the potential for data and algorithmic biases [40].

Despite the considerable magnitude of these challenges, both researchers and clinicians are actively engaged in endeavors to overcome them. Their concerted efforts aim to enhance the precision and dependability of AI models utilized in neurodisease detection. These efforts primarily revolve around leveraging AI techniques that contribute to achieving accurate diagnostic outcomes.

IV. MATERIALS AND METHOD

The methodologies we followed for this study are shown in Figure 1.

A. DATASET COLLECTION

1) DATASET 1

This research paper introduces a meticulously preprocessed dataset of MRI scans designed for the purpose of detecting AD. The dataset is conveniently accessible on the renowned open-source platform Kaggle [41], serving as a valuable resource for researchers in the field. The dataset comprises a total of 6400 images. These images have been sourced from diverse outlets, including hospitals, websites, and public repositories, ensuring a comprehensive representation of the disease. A few samples of each class (Mild Demented, Moderate Demented, Non Demented, and Very Mild Demented) from the dataset are shown in Figure 2.

To facilitate comprehensive analysis and investigation, the dataset has been thoughtfully partitioned into four distinct groups, with each group representing a specific stage of AD, ranging from mild to advanced dementia. The dataset employs a uniform T1-weighted imaging protocol for all MRI scans, guaranteeing a consistent and standardized approach to data acquisition, which enhances the comparability and reliability of the MRI data utilized in our study. The dataset details are presented in Table 1.

2) DATASET 2

In Dataset 2, we used a subset of Dataset 1, where the Dementia class was made up of the categories of Mild Demented, Moderate Demented, and Very Mild Demented. In contrast, the Non Demented class was renamed as Healthy. The rationale behind this selection was to create a simplified binary classification task for our model, which distinguishes

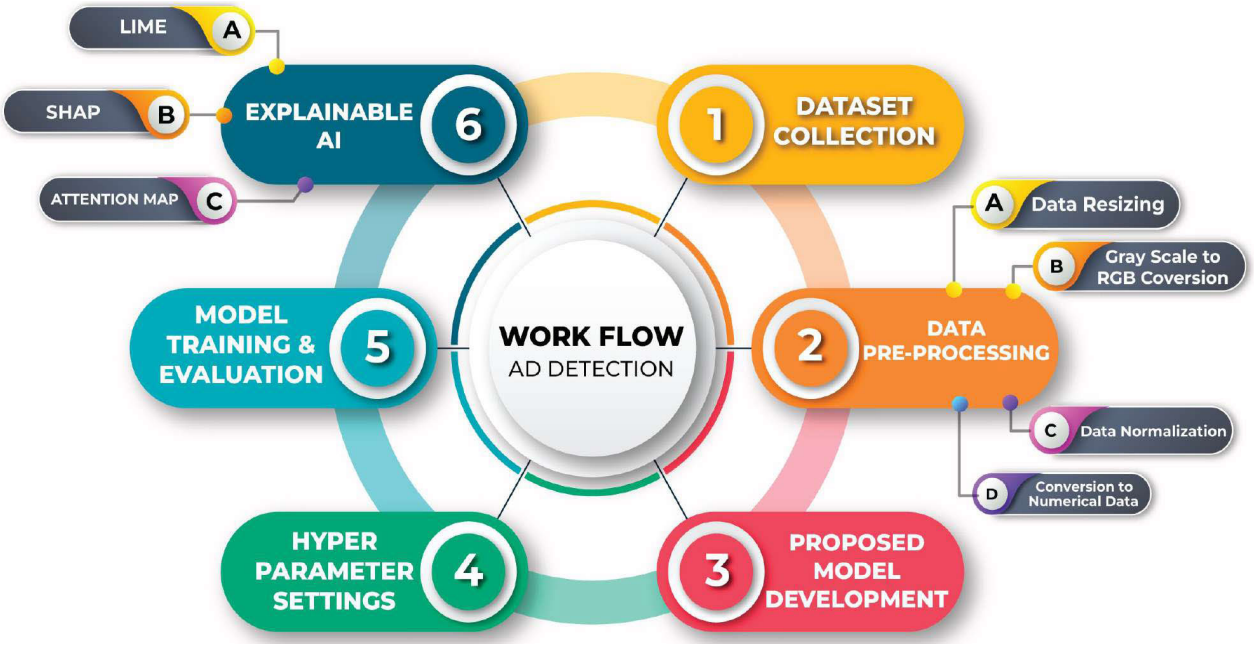

FIGURE 1. Workflow of the proposed methodology showcasing the sequential steps involved in the research process.

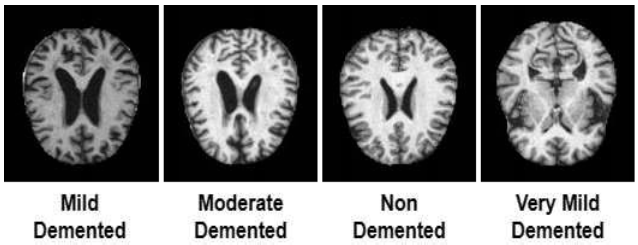

FIGURE 2. Sample images of the dataset 1.

FIGURE 3. Sample images of the dataset 3.

between individuals with some level of dementia and those without. This binary classification simplification allowed us to assess the model's ability to identify dementia cases effectively. This approach allowed for a simplified analysis and straightforward interpretation of the results. The details of datasets are shown in Table 1 as well. It is important to note that both datasets were examined and determined to be beneficial in attaining the objectives of the study.

3) DATASET 3

The research utilized data from the AD Neuroimaging Initiative (ADNI) database, specifically from the ADNI 1 baseline phase. Imaging procedures were conducted on a 3T system, employing an MRI T1 Weighted imaging protocol [42]. The dataset comprises information from 198 individual participants stored in Nifti format. Within this cohort, 41 participants are affected by AD, with 14 being male and 27 female. Mild Cognitive Impairment (MCI) is observed in 97 participants, including 57 males and 38 females. Additionally, 60 participants exhibit Common Normal (CN) conditions, with 22 males and 38 females. The mean age of participants diagnosed with AD is 74.07 years, with ages ranging from a minimum of 57 to a maximum of 89 years. For individuals with MCI, the mean age is 74.47 years, and their ages range from a minimum of 55 to a maximum of 88 years. On the other hand, CN participants have a mean age of 75.23 years, ranging from a minimum of 70 to a maximum of 86 years. Each patient's Nifti format was transformed into a set of 2D axial images to facilitate further analysis. A meticulous selection process was applied to streamline image processing algorithms, focusing on the central portion of the images–specifically, from the ventricular area to the hippocampus area, as it contains the most informative data [43], [44]. Non-relevant images, such as those including the skull or upper and lower brain regions, were manually excluded. From each participant, 14 to 16 slices of 2D axial images were extracted, resulting in a dataset comprising 2970 images, as illustrated in Figure 3. The resulting dataset is categorized into three groups: AD, MCI, and CN, containing 615, 1455, and 900 images, respectively. This information is summarized in Table 1, providing a comprehensive overview of the distribution of images across different diagnostic categories.

TABLE 1. Alzheimer's disease datasets used in this study.

Datasets	Label	Number of samples	Total
Dataset 1	Mild Demented	896	6400
	Moderate Demented	64	
	Non Demented	3200	
	Very Mild Demented	2240	
Dataset 2	Healthy	3200	6400
	Dementia	3200	
Dataset 3	Alzheimer's Disease	615	2970
	Mild Cognitive Impaired	1455	
	Common Normal	900	

TABLE 2. Hyperparameters of our proposed ViT-GRU model with its values.

Hyperparameters	Values
Epochs	20
Batch size	32
Image size	(128x128x3)
Learning rate	0.0001
Weight decay	0.0001
Optimizer	AdamW
Loss Function	Categorical cross-entropy
Patch size	8
Number of patches	256
Projection dimension	64
Number of parallel self-attention heads	4
Number of transformer encoder layers	8

B. DATA PREPOSSESSING

Data preprocessing is a fundamental and critical step in image classification tasks, as it ensures that the data is correctly prepared before feeding it into the model [31], [45]. Our dataset consists of grayscale (L) images, which we transformed into RGB format by replicating the grayscale channel three times. This conversion was necessary because most pre-trained CNNs are designed to work with RGB images. By converting the images to RGB format, we can leverage the knowledge learned by these pre-trained models. Furthermore, we performed rescaling on the RGB images to normalize the pixel values between 0 and 1. This normalization step is crucial as neural networks are sensitive to the scale of input data. Rescaling ensures that the model can effectively learn meaningful patterns from the data [6], [33]. In addition to the aforementioned preprocessing steps, we resized all images to a standardized dimension of 128 $\times$ 128. This resizing step ensures that all images have a consistent size, enabling the model to process them efficiently.

C. PROPOSED ViT-GRU MODEL

The proposed model for AD classification is a ViT-GRU architecture shown in Figure 4 is a novel DL model for AD detection, which combines the power of ViT [46] and GRU [47]. The model is designed to efficiently classify brain MRI images as healthy or affected by AD.

1) ViT FOR FEATURE EXTRACTION

Our model's primary component is the ViT, a cutting-edge architecture known for its exceptional ability to capture visual features from images using self-attention mechanisms. By adopting the ViT backbone, our model gains the capability to learn hierarchical representations of brain MRI images, effectively extracting crucial patterns and features indicative of AD. We removed the Multi-Layer Perceptron (MLP) layer to optimize the ViT encoder and incorporated layer normalization to stabilize training and facilitate faster convergence. We added a dropout layer to prevent overfitting and improve generalization. Lastly, we introduced a "flatten" layer to expand the model's capacity, enabling it to capture more diverse and intricate visual patterns from the MRI images, potentially improving AD detection performance.

2) GRU FOR TEMPORAL ANALYSIS

After the feature extraction stage, we introduce a GRU unit to perform temporal analysis on the extracted visual features. The GRU is a specific type of Recurrent Neural Network (RNN) known for its proficiency in capturing sequential patterns and dependencies within the data. By integrating the GRU with 1024 units, our model can effectively leverage the temporal dynamics in brain MRI images, thereby enhancing its ability to discern and classify AD with increased discriminative power.

3) CLASSIFICATION HEAD

A classification head is introduced at the end of the GRU layer to make the final prediction. The GRU's hidden state at the last time step is passed through fully connected layers, followed by a softmax activation function to obtain the probability distribution over classes.

D. HYPERPARAMETERS SETTINGS

The models we employed for our research boasted many parameters, opening up a vast landscape of potential architectural adjustments. As we optimized these models, our primary focus turned to hyperparameter tuning, a process essential for achieving peak performance. This entailed identifying hyperparameter values that closely approached the ones yielding the best possible results. To accomplish this, we delved into a repertoire of commonly used hyperparameter values, all while exploring innovative avenues to refine our model evaluation and prediction processes. Table 2 concisely records the hyperparameter values meticulously utilized throughout our proposed ViT-GRU model. Following our model architecture recommendations, 54,049,476 trainable

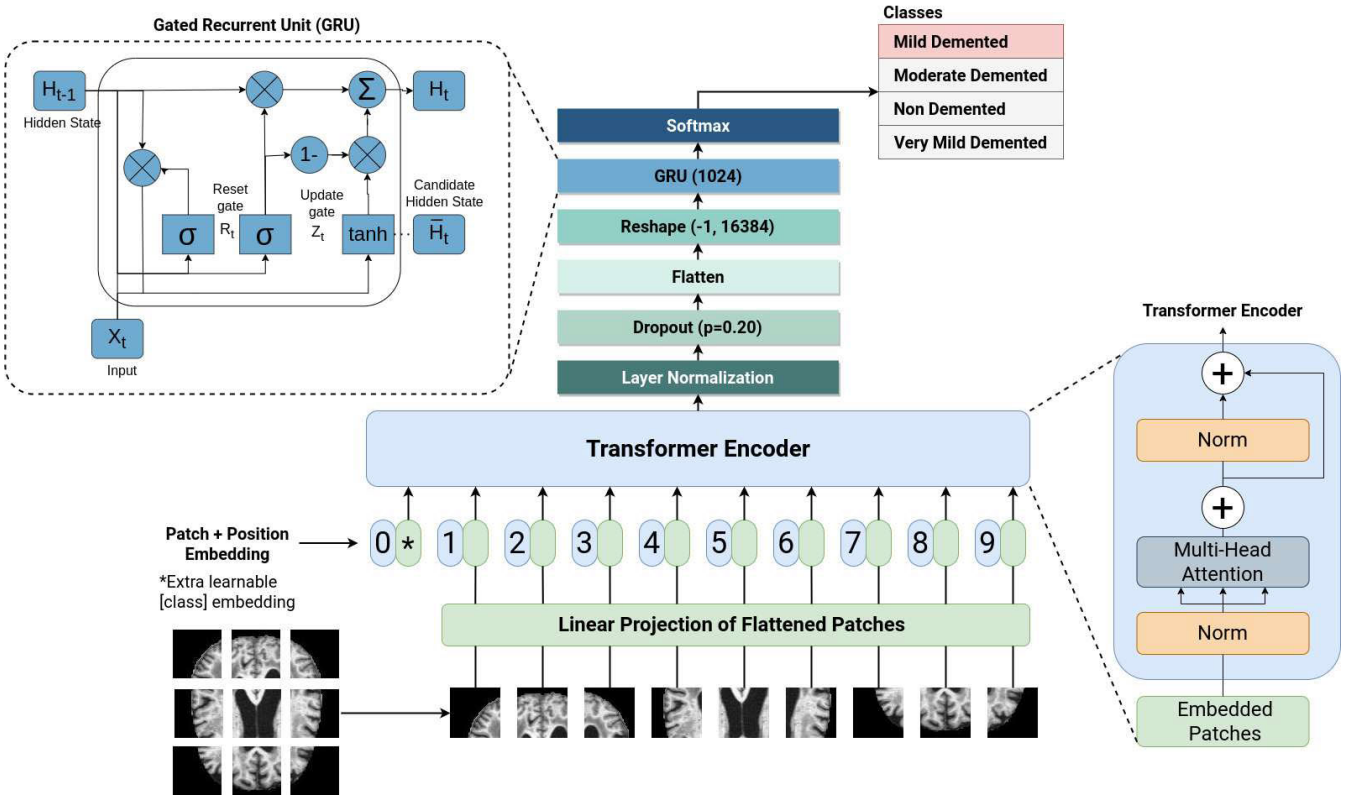

FIGURE 4. Architecture of the hybrid ViT-GRU model illustrating the interconnected components and their functional relationship in the proposed model.

parameters await estimation, with no single non-trainable parameter in sight.

The training was conducted on Google Colab using a GPU with 12 GB of RAM.

E. EVALUATION MATRIX

The proposed model's performance is evaluated using various metrics, including accuracy, precision, recall, F1-score, specificity, sensitivity, and Cohen's kappa. These metrics are derived from the information provided in the confusion matrix like True Positive (TP), True Negative (TN), False Positive (FP), and False Negative (FN), which represent the model's performance. The formula we calculated for the performances of our proposed ViT-GRU model is as follows:

$$Accuracy = \frac{TP + TN}{TP + TN + FP + FN} \tag{1}$$

$$Precision = \frac{TP}{TP + FP} \tag{2}$$

$$Recall = \frac{TP}{TP + FN} \tag{3}$$

$$F1 - score = 2 \times \frac{Precision \times Recall}{Precision + Recall} \tag{4}$$

$$Specificity = \frac{TN}{TN + FP} \tag{5}$$

$$\kappa = \frac{P_o - P_e}{1 - P_e} \tag{6}$$

where κ, P_o, and P_e represent Cohen's kappa value, the observed agreement between raters, and the expected agreement by chance, respectively.

F. EXPLAINABLE ARTIFICIAL INTELLIGENCE

XAI is an increasingly vital aspect of AI that aims to create AI systems that are transparent and easily understandable to humans. As AI models become more sophisticated and complex, understanding the reasoning behind their decisions becomes increasingly difficult. This creates potential issues in health care, where AI systems can make life-altering decisions. In the context of medical image classification, XAI is particularly crucial. By helping medical professionals understand and interpret AI system decisions, XAI can lead to more informed decisions about patient care and treatment plans. It is also essential for regulatory and ethical reasons, as regulators and medical organizations often require transparency in the decision-making process of AI systems in medical applications to ensure consistency with medical standards and regulations. Several explainable AI techniques, such as LIME, SHAP, and Attention map, have been applied to improve the interpretability and transparency of DL models used for AD detection. LIME generates heatmaps highlighting the essential regions of the medical images, and SHAP uses a game-theoretic approach to attribute the contribution of each input feature to the prediction. Attention Maps, on the other hand, provide insight into how the

model focuses on different regions of the image to make its decision. These techniques help to determine the essential features and areas in the medical images that contributed to the model's decision. This information can improve the diagnosis's accuracy and communication between medical professionals and patients.

1) LIME AS XAI

LIME is a powerful tool that can provide insight into the predictions made by ML models [48]. Unlike other interpretability methods, Model-agnostic means that LIME can be used with any ML model, regardless of its architecture or training algorithm. By generating a "heatmap," LIME helps identify the regions of an input image most important in a model's decision-making process. This heatmap is created by assigning a relative importance score to each pixel or area of a vision based on its contribution to the model's prediction. In our study, By examining the heatmap generated by LIME, we gained valuable insights into the crucial regions of the brain that contributed to the type of each image.

Using the top three features, we created a LIME heatmap that enabled us to validate the performance of our model and gain insights into the underlying patterns associated with the different classes of AD.

2) SHAP AS XAI

SHAP is a framework that enables the interpretation of ML model outputs, specifically by using Shapley values to explain the contribution of each feature to the model's output for a given input [49]. In the domain of medical image classification, SHAP can be utilized to identify the most significant regions of an image that are crucial for the model's classification decision. By using SHAP, important feature values are highlighted by red pixels, which indicate a higher probability of a particular class being predicted. In contrast, blue pixels denote features that reduce the likelihood of the expected type.

In the context of AD classification, we utilized SHAP to generate visual representations of the model's predictions, which validated the model's performance and provided additional insights into the critical regions of the brain for the classification task. We observed that the visual explanations produced by SHAP complemented those generated by LIME, providing a more comprehensive understanding of the underlying patterns in the data.

3) ATTENTION MAP AS XAI

An attention map is a technique used in XAI to visualize the regions of an input image that a DL model focuses on during classification or segmentation tasks. By highlighting the relevant regions, the attention map provides insights into the model's decision-making process, making it more interpretable and transparent.

In medical image classification, attention maps can be used to identify the specific regions of the brain affected by AD. Jet color attention maps often represent the different activation levels in the highlighted regions. The color scheme ranges from blue (low activation) to red (high activation), with green and yellow representing intermediate activation levels. The last multi-head attention layer in a ViT-GRU model is used to plot the attention map because it captures the most relevant features for the final classification decision. The attention weights obtained from this layer highlight the most relevant regions of the input image, making it easier to interpret the model's decision-making process. Therefore, visualizing the attention map from the last multi-head attention layer can improve our understanding of how the model works.

V. RESULTS

In the initial experiment, a 10-fold cross-validation strategy was employed. This method divides the dataset into ten equal parts, commonly called "folds." During each iteration or fold, nine of these folds are used for training, constituting 90% of the data, while the remaining one fold, comprising 10% of the data, is reserved for testing. This process is repeated ten times, with each fold taking on the role of the test set once.

Before each fold's training phase begins, an additional step is introduced. 10% of the training data is further set aside for validation. This subset, known as the validation set, is used to fine-tune the model's hyperparameters and monitor its performance during training. This rigorous validation ensures the model is fine-tuned to its optimal configuration before being tested on the test fold.

In a distinct experiment referred to as Experiment 2, the dataset was split into three sets, constituting 80% for training, 10% for testing, and 10% for validation. This division was achieved by shuffling the data with different seeds. It is important to note that we opted to train the model from scratch. This decision was made to ensure that previous training iterations did not influence the model's performance and to evaluate its capability to generalize to different experimental conditions.

Several pre-trained CNN models were incorporated into the study to evaluate the performance of machine learning models. These models have been pre-trained on large-scale datasets and are known for extracting intricate features from images, making them ideal candidates for various computer vision tasks.

A. RESULTS OF DATASET 1

In our rigorous analysis of Dataset 1, we employed a 10-fold cross-validation strategy to evaluate the performance of our model thoroughly. The results, elegantly summarized in Table 3, paint a vivid picture of our model's exceptional capabilities. First and foremost, our model showcased its precision with a remarkable mean precision score of 99.54%. This indicates its proficiency in accurately identifying positive cases within the dataset. Additionally, our model demonstrated an impressive recall rate of 99.53%, signifying its ability to capture actual positive instances effectively

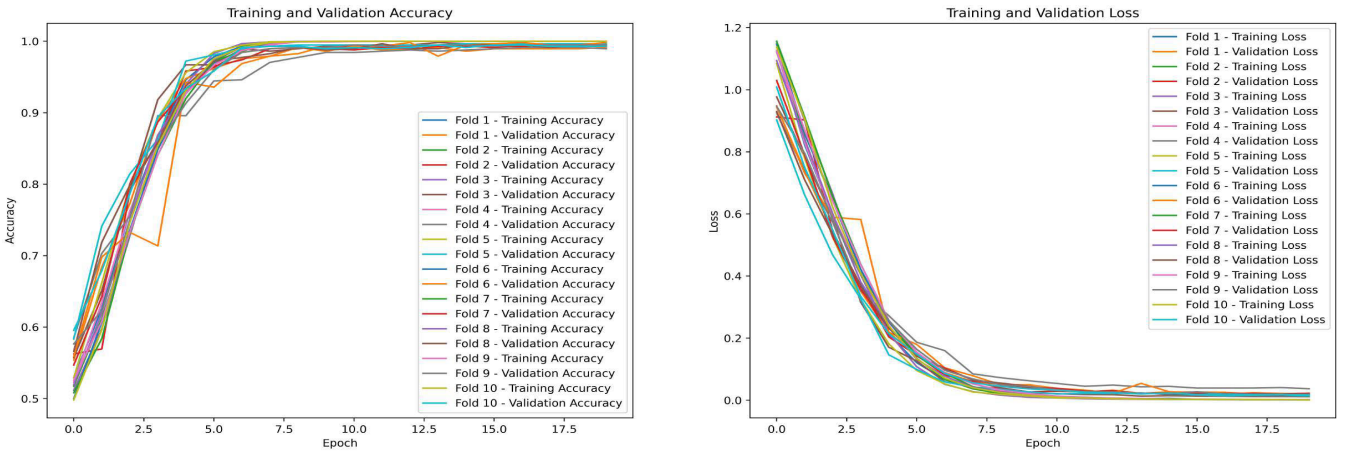

FIGURE 5. Accuracy and loss curves for 10 fold cross-validation on dataset 1.

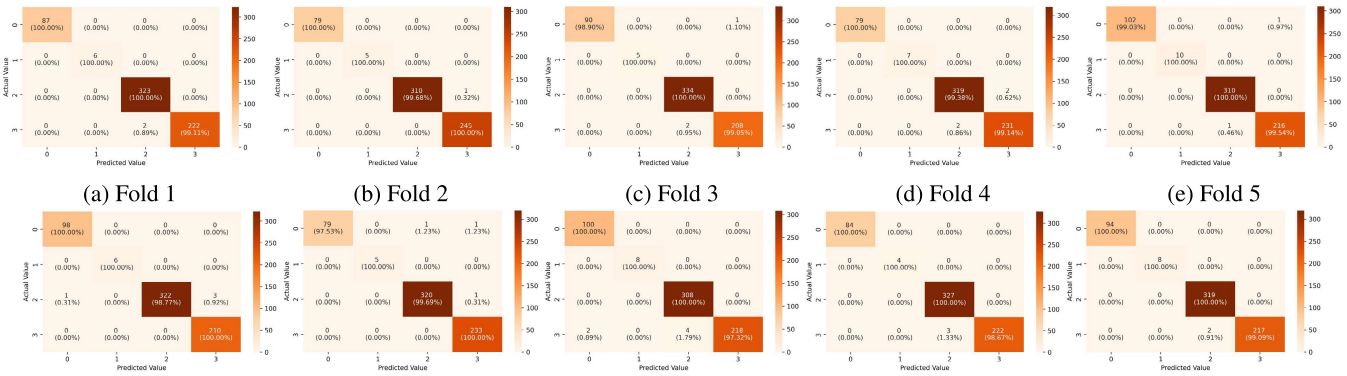

(a) Fold 1 (b) Fold 2 (c) Fold 3 (d) Fold 4 (e) Fold 5

(f) Fold 6 (g) Fold 7 (h) Fold 8 (i) Fold 9 (j) Fold 10

FIGURE 6. Confusion matrices for 10 fold cross-validation on dataset 1 where 0, 1, 2, and 3 represent mild demented, moderate demented, non demented, and very mild demented, respectively.

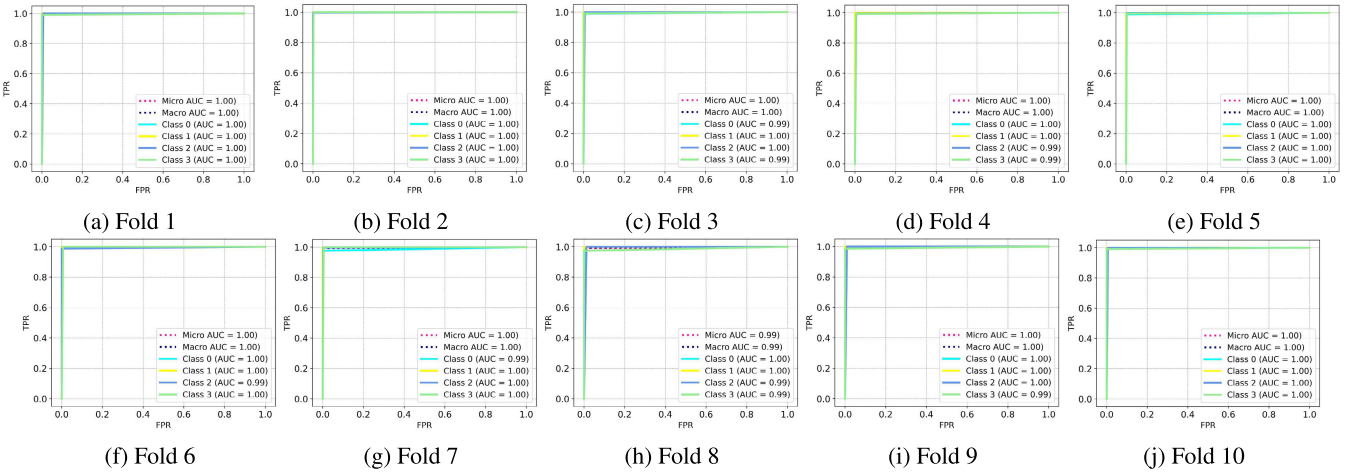

(a) Fold 1 (b) Fold 2 (c) Fold 3 (d) Fold 4 (e) Fold 5

(f) Fold 6 (g) Fold 7 (h) Fold 8 (i) Fold 9 (j) Fold 10

FIGURE 7. AUC-ROC curves for 10-fold cross-validation on dataset 1 where 0, 1, 2, and 3 represent mild demented, moderate demented, non demented, and very mild demented, respectively.

while minimizing false negatives. The F1-score, a metric that balances precision and recall, stood at an impressive 99.53%, underscoring the robustness of our model's performance. Moreover, the model excelled in specificity, achieving a score of 99.76%, which means it was adept at distinguishing negative cases with minimal false positives. Cohen's Kappa

TABLE 3. Results of 10 fold cross-validation on the dataset 1.

Number of fold	Precision(%)	Recall(%)	F1-score(%)	Specificity(%)	Cohen's Kappa	Test accuracy(%)
Fold 1	99.69	99.69	99.69	100	99.48	99.69
Fold 2	99.84	99.84	99.84	99.75	99.74	99.84
Fold 3	99.53	99.53	99.53	99.77	99.22	99.53
Fold 4	99.38	99.38	99.38	99.51	98.96	99.38
Fold 5	99.69	99.69	99.69	99.76	99.50	99.69
Fold 6	99.38	99.38	99.38	99.30	98.98	99.38
Fold 7	99.53	99.53	99.53	99.51	99.22	99.53
Fold 8	99.08	99.06	99.06	100	98.49	99.06
Fold 9	99.54	99.53	99.53	100	99.22	99.53
Fold 10	99.69	99.69	99.69	100	99.49	99.69
Mean	**99.54**	**99.53**	**99.53**	**99.76**	**99.23**	**99.53**

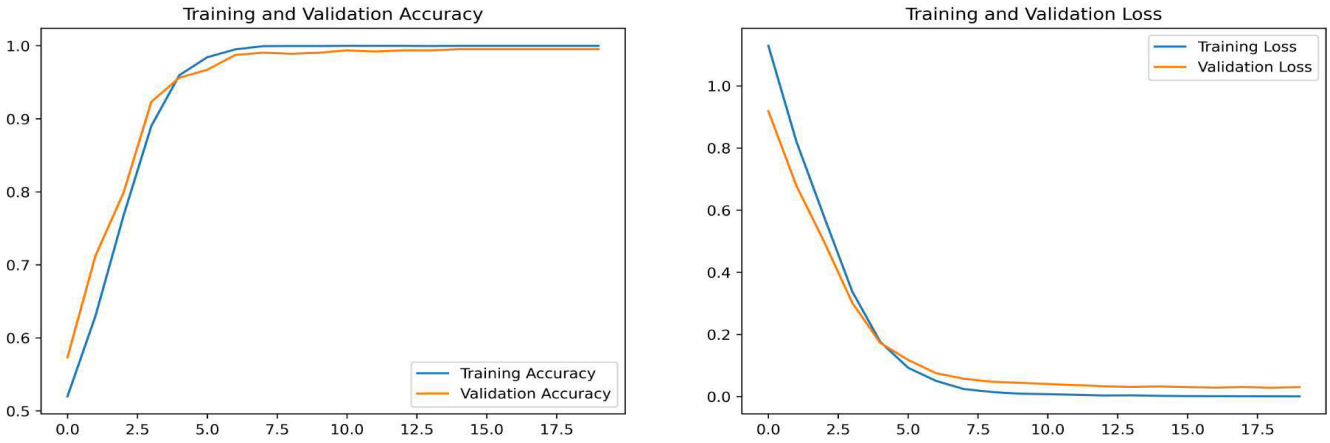

FIGURE 8. Accuracy and loss curve for dataset 1 in experiment 2.

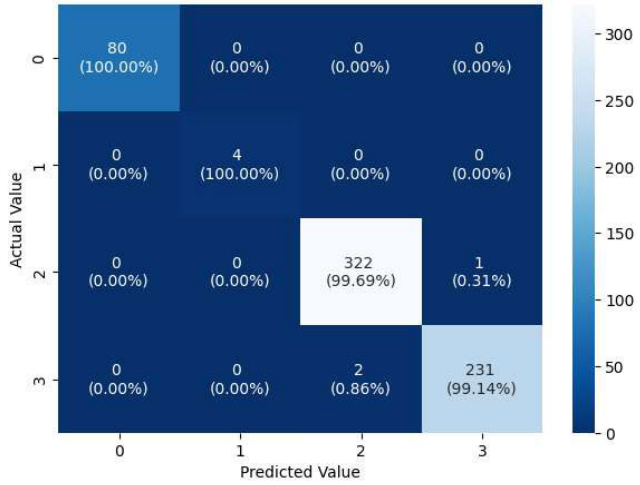

FIGURE 9. Confusion matrix for dataset 1 in experiment 2 where 0, 1, 2, and 3 represent mild demented, moderate demented, non demented, and very mild demented, respectively.

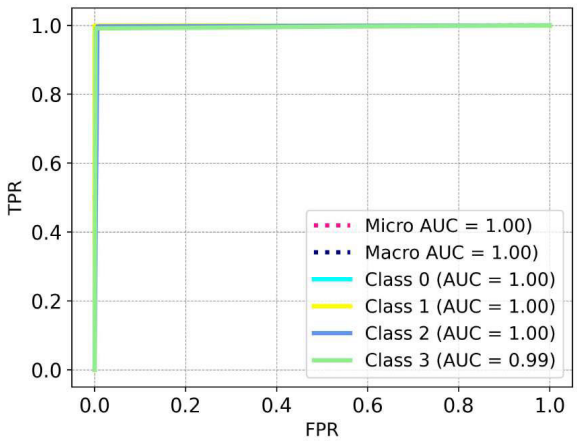

FIGURE 10. AUC-ROC curves for dataset 1 in experiment 2 where 0, 1, 2, and 3 represent mild demented, moderate demented, non demented, and very mild demented, respectively.

value, a measure of agreement beyond chance, was equally impressive at 99.23%, highlighting the reliability of our model's predictions. Lastly, the mean test accuracy of 99.53% further corroborates the model's ability to classify data points accurately. To provide a more holistic perspective of our experiments, we complemented these numerical results with visual aids. Figure 5, for instance, illustrates the training accuracy and loss curve across the various folds, providing insights into our model's learning process. In Figure 6,

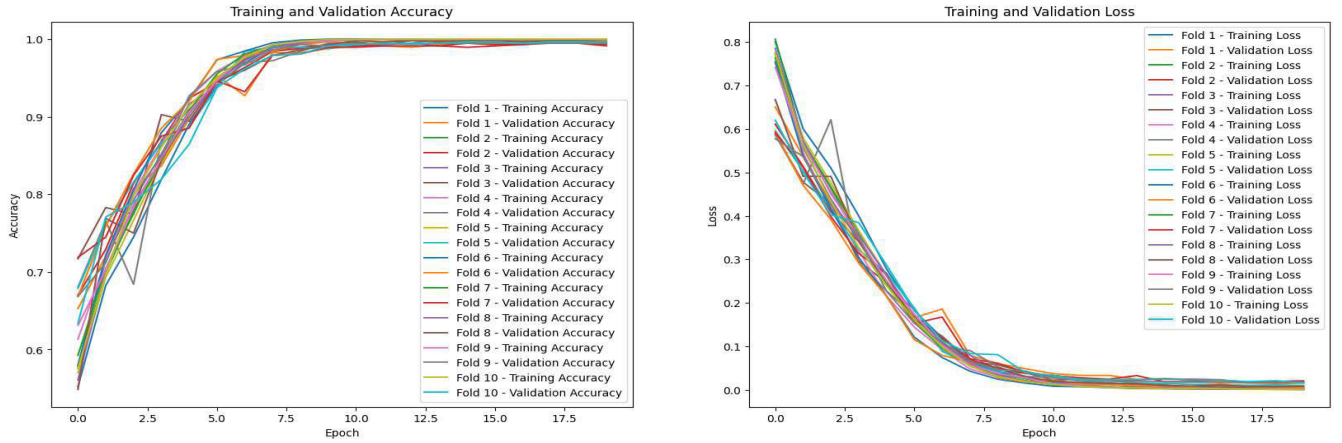

FIGURE 11. Accuracy and loss curves for 10 fold cross-validation on dataset 2.

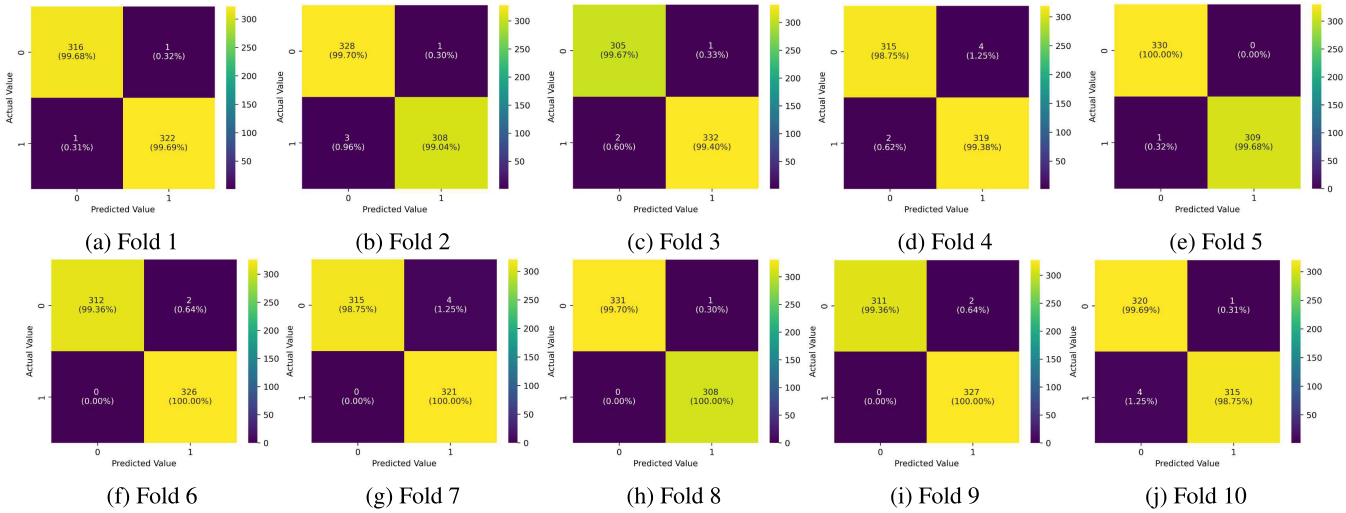

(a) Fold 1 (b) Fold 2 (c) Fold 3 (d) Fold 4 (e) Fold 5

(f) Fold 6 (g) Fold 7 (h) Fold 8 (i) Fold 9 (j) Fold 10

FIGURE 12. Confusion matrices for 10-fold cross-validation on dataset 2 where 0 and 1 represent dementia and healthy, respectively.

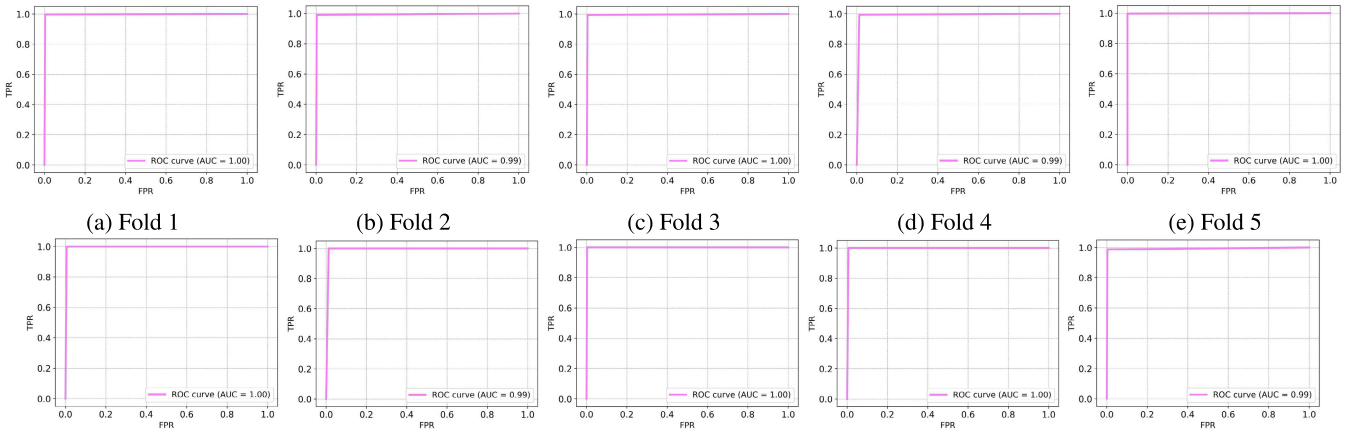

(a) Fold 1 (b) Fold 2 (c) Fold 3 (d) Fold 4 (e) Fold 5

(f) Fold 6 (g) Fold 7 (h) Fold 8 (i) Fold 9 (j) Fold 10

FIGURE 13. AUC-ROC curves for 10 fold cross-validation on dataset 2.

we present the confusion matrix for each fold, offering a detailed breakdown of its classification performance. Furthermore, Figure 7 showcases the Area Under the Receiver Operating Characteristic Curves (AUC-ROC)

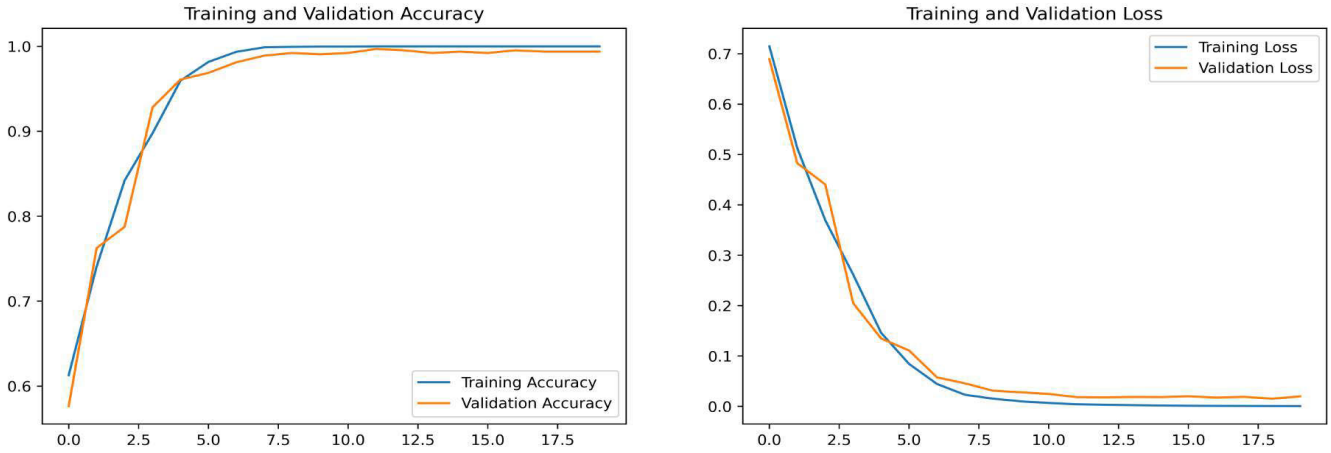

FIGURE 14. Accuracy and loss curve for dataset 2 in experiment 2.

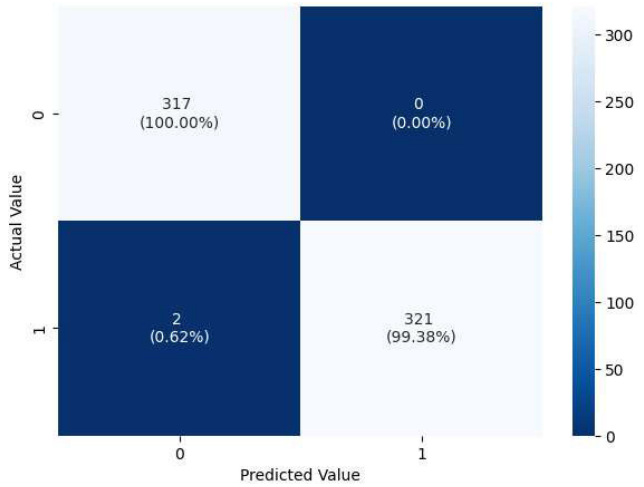

FIGURE 15. Confusion matrix for Dataset 2 in experiment 2 where 0 and 1 represent dementia and healthy, respectively.

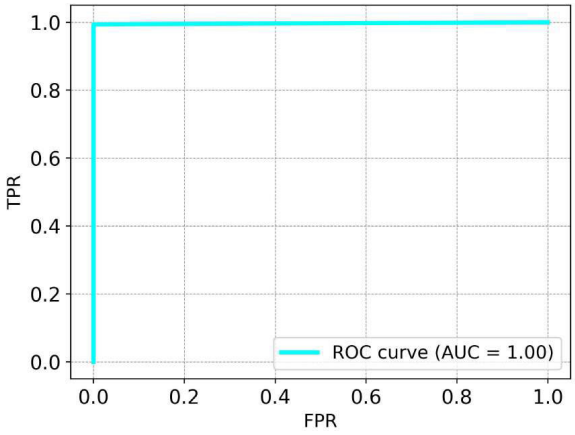

FIGURE 16. AUC-ROC curve for dataset 2 in experiment 2.

for each fold, demonstrating the model's discrimination capabilities.

In Experiment 2, our model consistently achieved high precision, recall, and F1-score, all at 99.53%. The Cohen's Kappa value also stood at 99.23, with a specificity of 99.76%. The training duration was 450.98 seconds. The test accuracy is also at 99.53%. Figure 9 provided an in-depth analysis of the confusion matrix, while Figure 10 illustrated the AUC-ROC curves, collectively reaffirming the model's excellence across various experimental setups.

B. RESULTS OF DATASET 2

In the context of Dataset 2, we conducted a comprehensive analysis using 10-fold cross-validation. Our model consistently demonstrated remarkable performance metrics, with an average precision, recall, and F1-score of 99.53% and an impressive specificity of 99.47%. The Cohen's Kappa coefficient, a measure of agreement, was also relatively high at 99.06%. Additionally, the mean test accuracy stood at a remarkable 99.53%, as detailed in Table 4. Figure 11 illustrates the accuracy loss curves for each fold to visualize the performance further, offering insights into the model's training process. Figure 12 presents the confusion matrices for each fold, providing a detailed view of how the model classified different classes. Furthermore, Figure 13 showcased the AUC-ROC curves for each fold, indicating the model's ability to distinguish between types.

In Experiment 2, elevated precision, recall, and F1-score levels, registering at 99.69%. Furthermore, the Cohen's Kappa value was recorded at 99.37, with a corresponding specificity of 99.68%. The training process lasted for 432.08 seconds. The test accuracy mirrored the high performance, also resting at 99.69%. Figure 15 delved into the confusion matrix, providing a detailed view of the model's classification performance. Figure 16 depicts the AUC-ROC curve, reaffirming the model's excellence in binary classification by effectively distinguishing between the two classes.

TABLE 4. Results of 10 fold cross-validation on the dataset 2.

Number of fold	Precision(%)	Recall(%)	F1-score(%)	Specificity(%)	Cohen's Kappa	Test accuracy(%)
Fold 1	99.69	99.69	99.69	99.68	99.37	99.69
Fold 2	99.38	99.38	99.37	99.70	98.75	99.38
Fold 3	99.53	99.53	99.53	99.67	99.06	99.53
Fold 4	99.06	99.06	99.06	98.75	98.12	99.06
Fold 5	99.84	99.84	99.84	100	99.69	99.84
Fold 6	99.69	99.69	99.69	99.36	99.37	99.69
Fold 7	99.38	99.38	99.37	98.75	98.75	99.38
Fold 8	99.84	99.84	99.84	99.70	99.69	99.84
Fold 9	99.69	99.69	99.69	99.36	99.37	99.69
Fold 10	99.22	99.22	99.22	99.69	98.44	99.22
Mean	**99.53**	**99.53**	**99.53**	**99.47**	**99.06**	**99.53**

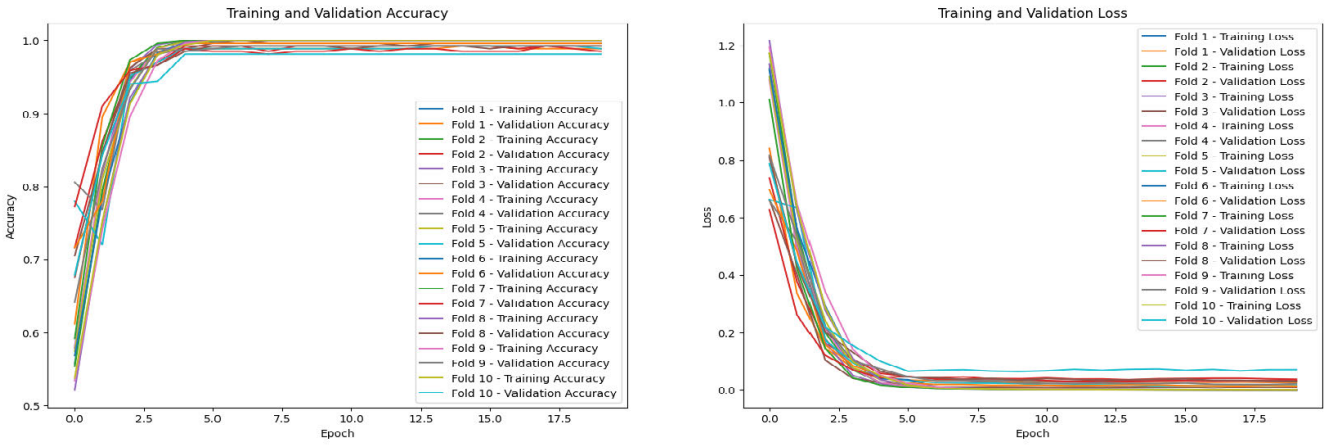

FIGURE 17. Accuracy and loss curves for 10 fold cross-validation on dataset 3.

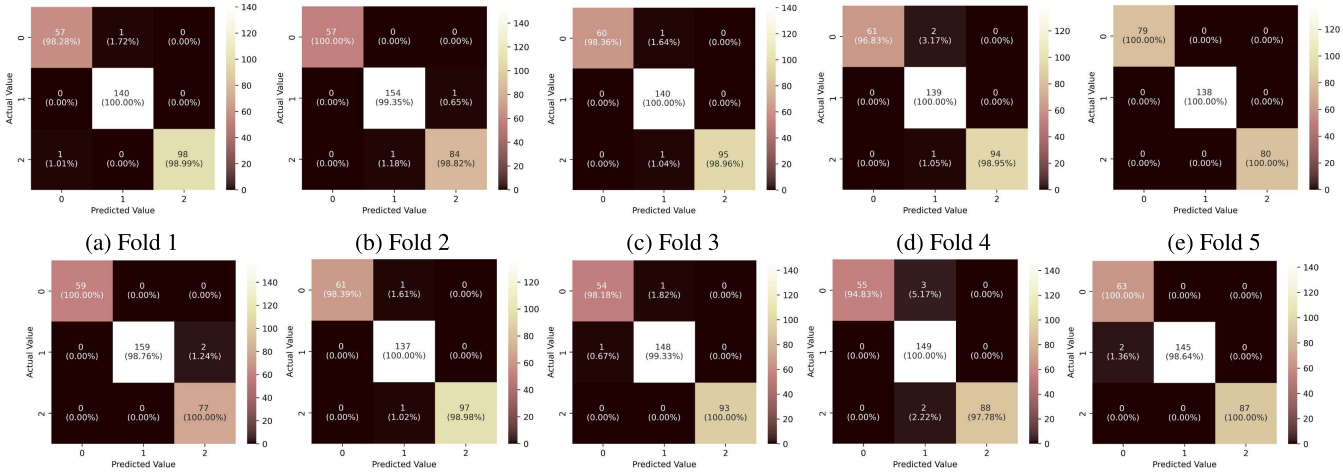

(a) Fold 1 (b) Fold 2 (c) Fold 3 (d) Fold 4 (e) Fold 5

(f) Fold 6 (g) Fold 7 (h) Fold 8 (i) Fold 9 (j) Fold 10

FIGURE 18. Confusion matrices for 10-fold cross-validation on dataset 3 where 0, 1, and 2 represent AD, MCI, and CN, respectively.

C. RESULTS OF DATASET 3

In the context of Dataset 3, our model consistently demonstrated exceptional performance across multiple evaluations. During K-fold cross-validation, it consistently achieved outstanding metrics, with an average precision, recall, and F1-score of 99.26% and an impressive specificity of 99.45%. The Cohen's Kappa coefficient, indicating the model's agreement with actual values, was also notably

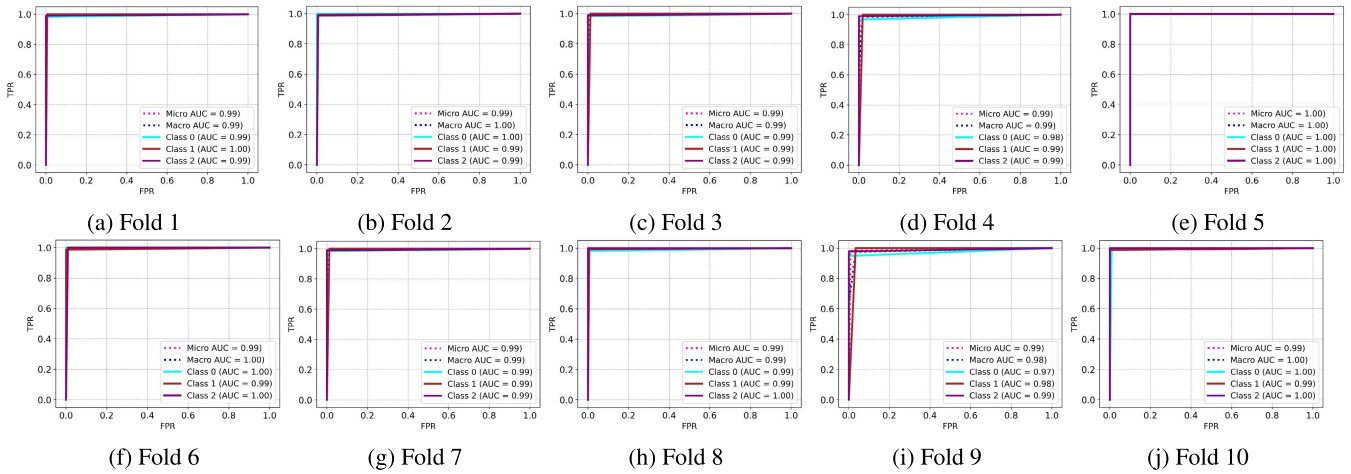

FIGURE 19. AUC-ROC curves for 10-fold cross-validation on dataset 3 where 0, 1, and 2 represent AD, MCI, and CN, respectively.

TABLE 5. Results of 10 fold cross-validation on the dataset 3.

Number of fold	Precision(%)	Recall(%)	F1-score(%)	Specificity(%)	Cohen's Kappa	Test accuracy(%)
Fold 1	99.33	99.33	99.33	100	98.93	99.33
Fold 2	99.33	99.33	99.33	99.53	98.89	99.33
Fold 3	99.34	99.33	99.33	100	98.93	99.33
Fold 4	99.01	98.99	98.99	100	98.40	98.99
Fold 5	100	100	100	100	100	100
Fold 6	99.34	99.33	99.33	99.09	98.88	99.33
Fold 7	99.34	99.33	99.33	100	98.94	99.33
Fold 8	99.33	99.33	99.33	100	98.91	99.33
Fold 9	98.37	98.32	98.31	100	97.26	98.32
Fold 10	99.35	99.33	99.33	100	99.92	99.33
Mean	**99.27**	**99.26**	**99.26**	**99.45**	**98.81**	**99.26**

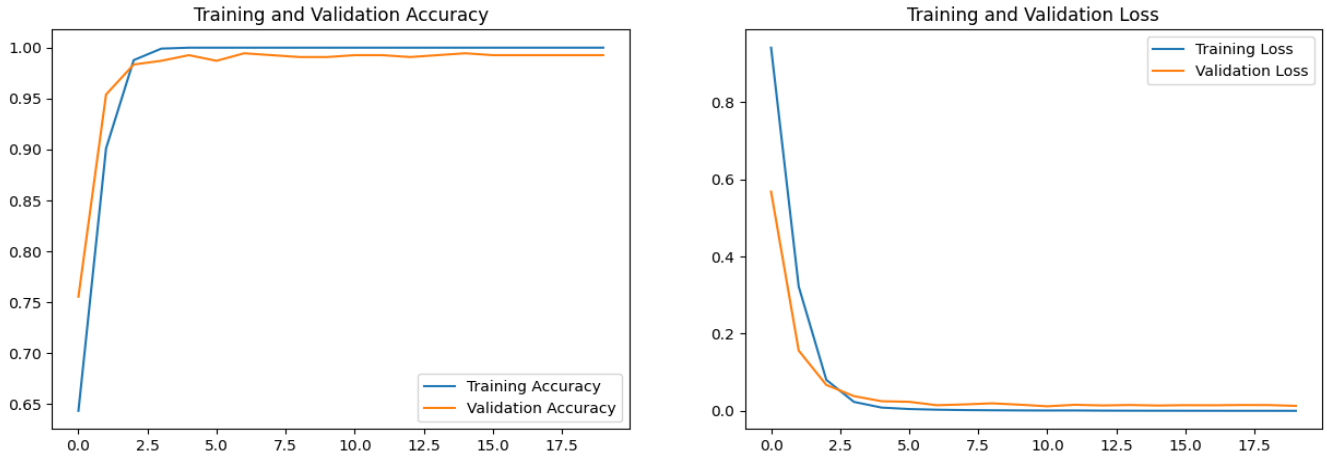

FIGURE 20. Accuracy and loss curve for dataset 3 in experiment 2.

high at 98.81%. Furthermore, the model showcased an exceptional mean test accuracy of 99.26%, as indicated in Table 5. Visual insights from Figure 17 displayed accuracy loss curves for each fold. In contrast, Figure 18 depicted confusion matrices, and Figure 22 presented AUC-ROC curves, highlighting the model's robustness and ability to

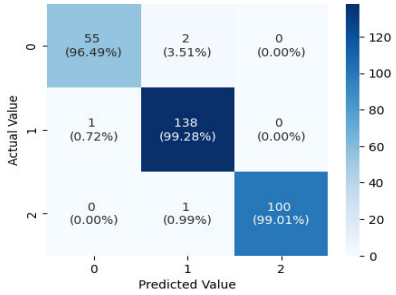

FIGURE 21. Confusion matrix for dataset 3 in experiment 2 where 0, 1, and 2 represent AD, MCI, CN, respectively.

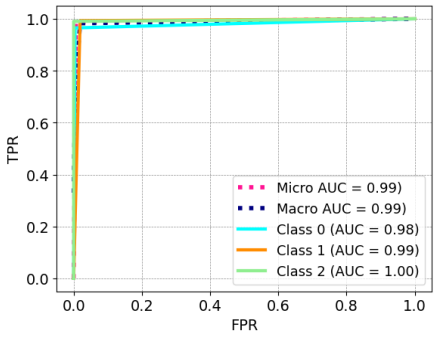

FIGURE 22. AUC-ROC curves for dataset 3 in experiment 2 where 0, 1, and 2 represent AD, MCI, CN, respectively.

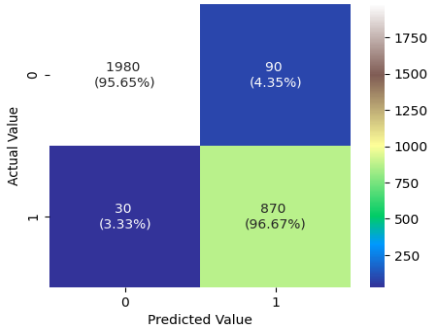

FIGURE 23. Confusion matrix for a model trained on dataset 2 and assessed on the holdout dataset from dataset 3 here 0 and 1 represents dementia and CN, respectively.

distinguish between different data classes. When applying 10-fold cross-validation without manually selecting slices, the model yielded a mean precision of 98.28%, recall of 98.18%, F1-score of 98.13%, specificity of 99.09%, Cohen's kappa of 96.83, and test accuracy of 98.18%.

In Experiment 2, precision is sustained at 98.66%, recall at 98.65%, F1-score at 98.65%, and Cohen's Kappa value at an impressive 97.85%, accompanied by an exceptional specificity of 100%. Once more, the test accuracy reached a remarkable 98.65%. Figure 20 provided insight into the accuracy and loss curves. Figures 21 and 22 provided valuable insights into the model's performance under different experimental setups, with Figure 21 offering detailed classification performance through confusion matrices and

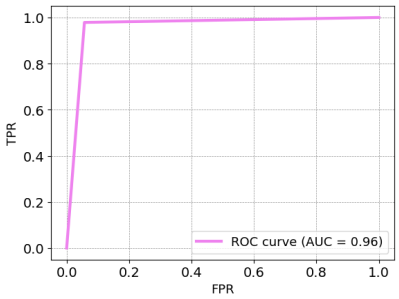

FIGURE 24. AUC-ROC curve for a model trained on dataset 2 and assessed on the holdout dataset from dataset 3.

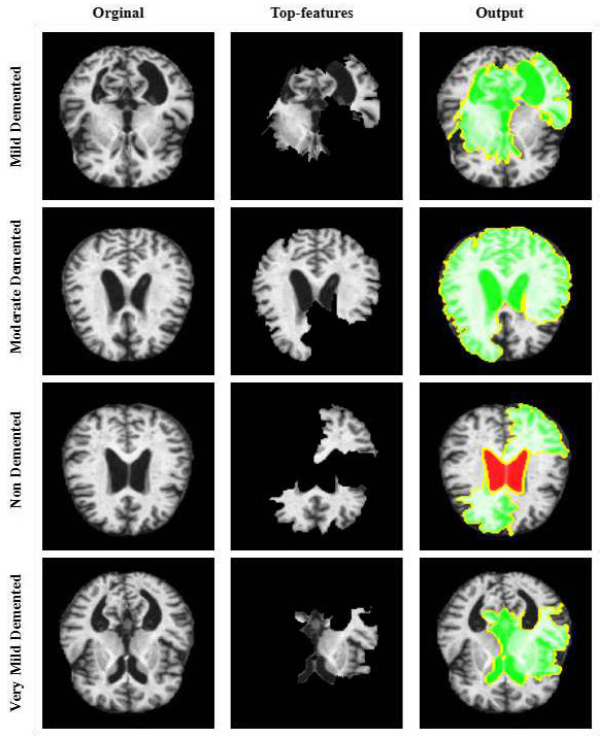

FIGURE 25. LIME for dataset 1 (Top three features).

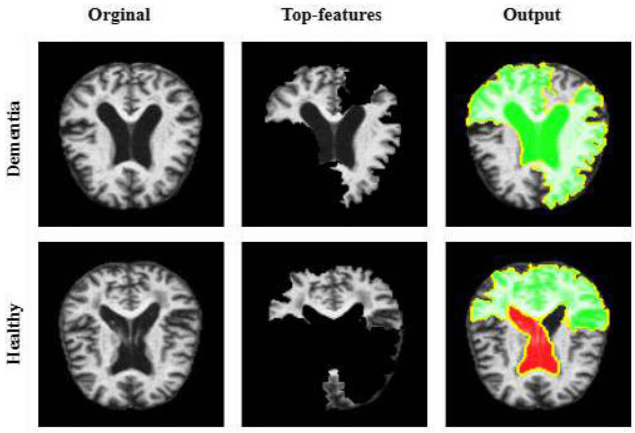

FIGURE 26. LIME for dataset 2 (Top three features).

Figure 22 reaffirming its excellence through the AUC-ROC curves.

TABLE 6. Comparing results of pre-trained CNN models with the proposed ViT-GRU on dataset 1.

Model	Optimizers	Precision(%)	Recall(%)	F1-score(%)	Specificity(%)	Cohen's Kappa	Time(Seconds)	Test accuracy(%)
ResNet50	AdamW	71.42	67.34	63.39	95.51	41.38	470.34	67.34
MobileNetV2	AdamW	95.48	95.47	95.45	97.52	92.39	450	95.47
VGG19	AdamW	90.11	89.53	89.34	97.75	82.24	670.19	89.53
Xception	AdamW	84.76	84.06	84.15	86.86	73.76	504.31	84.06
InceptionV3	AdamW	88.17	87.97	87.98	89.90	79.88	520.51	87.97
DenseNet121	AdamW	95.35	95.31	95.30	97.77	92.16	555.32	95.31
VGG16	AdamW	91.17	90.78	90.82	90.27	84.57	550.12	90.78
Proposed Model	AdamW	**99.53**	**99.53**	**99.53**	**99.76**	**99.23**	**450.98**	**99.53**

TABLE 7. Comparing results of pre-trained CNN models with the proposed ViT - GRU on dataset 2.

Model	Optimizers	Precision(%)	Recall(%)	F1-score(%)	Specificity(%)	Cohen's Kappa	Time(Seconds)	Test accuracy(%)
ResNet50	AdamW	77.66	77.66	77.66	77.92	55.31	475.29	77.66
MobileNetV2	AdamW	95.67	95.62	95.62	97.16	91.25	465.34	95.62
VGG19	AdamW	91.39	90.16	90.09	98.74	80.34	501.15	90.16
Xception	AdamW	88.92	88.44	88.39	82.65	76.85	490.09	88.44
InceptionV3	AdamW	91.88	91.88	91.87	91.48	83.75	487.54	91.88
DenseNet121	AdamW	94.06	93.44	93.42	99.37	86.89	480.17	93.44
VGG16	AdamW	94.06	93.91	93.90	96.85	87.82	558.23	93.91
Proposed Model	AdamW	**99.69**	**99.69**	**99.69**	**99.68**	**99.37**	**432.08**	**99.69**

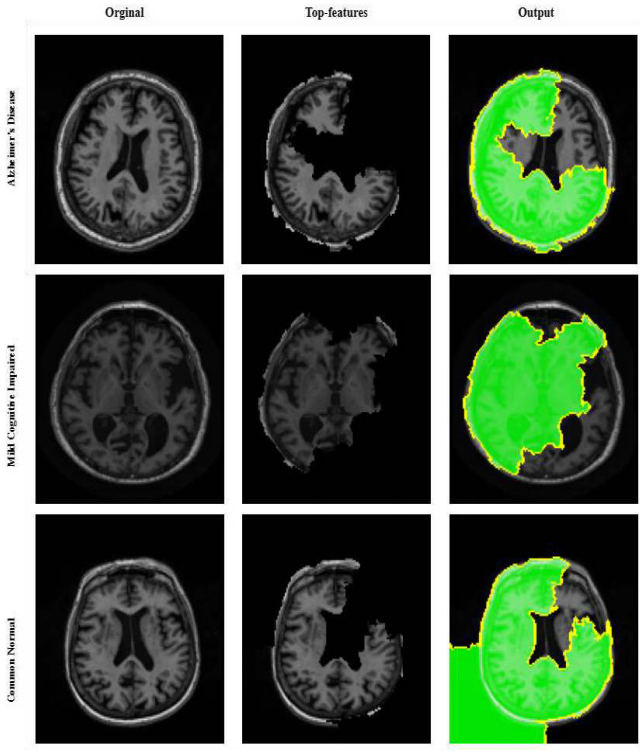

FIGURE 27. LIME for dataset 3 (Top three features).

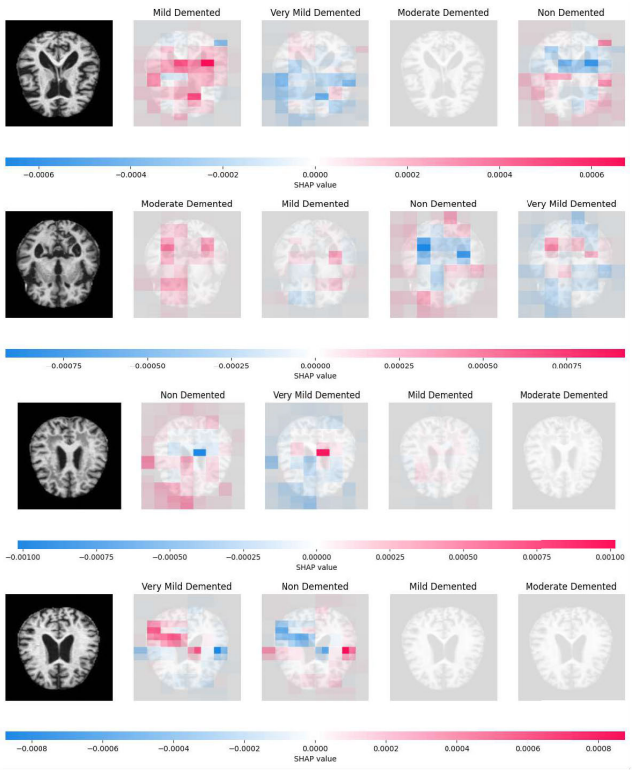

FIGURE 28. SHAP for dataset 1.

We also used this dataset as a holdout dataset for a model trained on dataset 2 for binary classification. In this evaluation, we merged two classes from the original 3-class dataset, namely AD and MCI, into a single dementia class, while CN remained unchanged. The model's performance for binary classification was assessed, resulting in a precision of 96.12%, a recall of 95.96%, an F1-score of 96.00%, a specificity of 95.65%, a Cohen's kappa of 90.61, and a test accuracy of 95.96%. The confusion matrix and AUC-ROC curve are shown in Figures 23 and 24, respectively.

VI. DISCUSSION

The accurate and early diagnosis of AD is critical for effective clinical intervention and management. In this study, we proposed a framework that combines a ViT and a GRU to detect AD characteristics from MRI images. ViT excels at extracting intricate features from brain images, capturing essential patterns relevant to AD. This gives our model a potent data representation. The GRU, an RNN, is adept at capturing sequential dependencies within these features.

TABLE 8. Comparing results of pre-trained CNN models with the proposed ViT - GRU on dataset 3.

Model	Optimizers	Precision(%)	Recall(%)	F1-score(%)	Specificity(%)	Cohen's Kappa	Time(Seconds)	Test accuracy(%)
ResNet50	AdamW	80.81	80.81	80.46	90.34	68.80	370.23	80.81
MobileNetV2	AdamW	97.00	96.98	96.98	97.45	95.79	310.31	96.98
VGG19	AdamW	97.15	96.97	96.94	100	95.12	420.12	96.97
Xception	AdamW	93.52	93.27	93.29	99.47	89.27	350.06	93.27
InceptionV3	AdamW	91.53	91.58	91.44	95.70	86.46	360.09	91.58
DenseNet121	AdamW	97.03	96.97	96.95	98.43	95.15	380.17	96.97
VGG16	AdamW	97.09	96.97	96.96	99.48	95.14	402.46	96.97
Proposed Model	AdamW	**98.66**	**98.65**	**98.65**	**100**	**97.85**	**289.67**	**98.65**

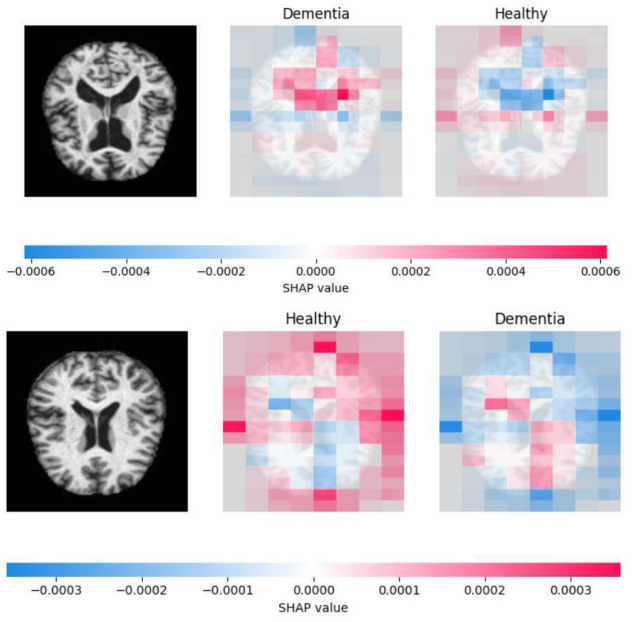

FIGURE 29. SHAP for dataset 2.

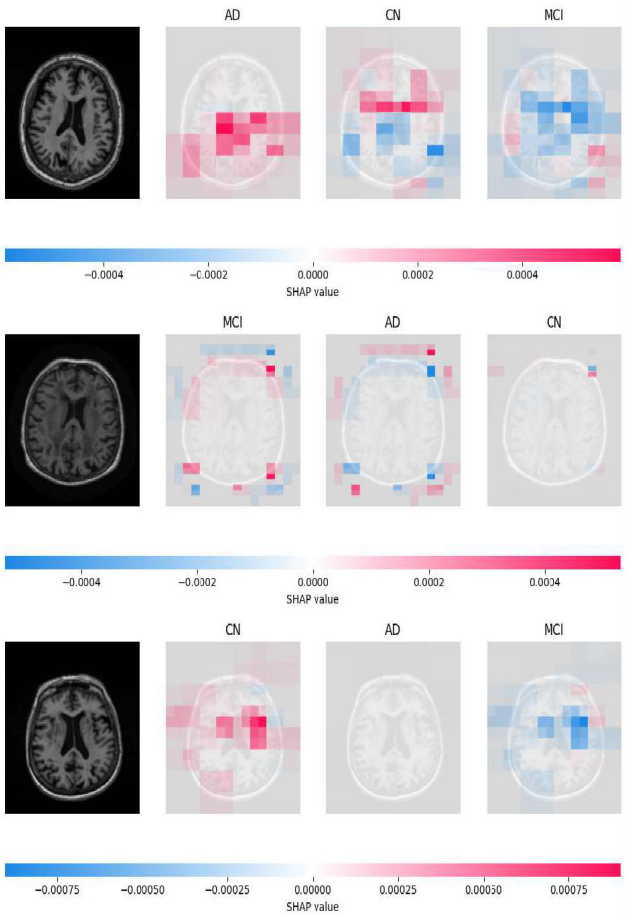

FIGURE 30. SHAP for dataset 3.

This is vital because Alzheimer's progression unfolds over time, and the GRU effectively handles such temporal data. Unlike CNNs, which focus on spatial features, our ViT-GRU model captures temporal dependencies in brain imaging data, contributing to its superior performance. Furthermore, our approach leverages ViT's self-attention mechanisms, enabling us to pinpoint crucial brain regions or patterns that drive the model's predictions. This enhances the model's explainability, a valuable aspect of AD detection. The model's performance in classification tasks was exceptional, with accuracy rates of 99.53%, 99.69%, and 99.26% for Dataset 1, Dataset 2, and Dataset 3, respectively. When Dataset 3 was tested on a model trained on Dataset 2, the accuracy was 95.96%. These impressive results demonstrate the model's effectiveness.

Our comprehensive study involved an in-depth analysis utilizing several pre-trained DL models, namely ResNet50, MobileNetV2, VGG19, Xception, InceptionV3, DenseNet121, and VGG16. We fine-tuned these models by adjusting hyperparameters, incorporating dense layers after the flatten layer, and, in some cases, unfreezing the last few layers to achieve the highest accuracy. Our primary objective was to assess their performance across key metrics such as precision, recall, F1-score, specificity, Cohen's Kappa, training time, and test accuracy. Furthermore, we introduced and evaluated our own proposed model, which outperformed all other models in every measured aspect and demonstrated significantly reduced training time. Tables 6, 7, and 8 present the comparative results for Dataset 1, Dataset 2, and Dataset 3.

Incorporating XAI techniques into our model enhances its interpretability, a crucial factor for its acceptance and integration into clinical practice. By providing clinicians with insights into the model's decision-making process, we enable them to understand the factors that contribute to the AD diagnosis. This transparency fosters trust in the model and allows clinicians to validate its decisions, ensuring that the

TABLE 9. Comparative assessment of prior studies.

Study	Year	Model	Dataset	Image modalities	Number of class	Number of images	Performance	XAI
Basaia et al. [19]	2019	Deep neural networks	ADNI	MRI	2	825	Accuracy: 99.20% Precision: — Recall: — F1-score: —	Not used
Wang et al. [51]	2019	3D densely connected convolutional network	ADNI	MRI	2	530	Accuracy: 98.83% Precision: 98.70% Recall: 98.70% F1-score: —	Not used
Acharya et al. [52]	2021	Transfer Learning (TL)	AD dataset kaggle	MRI	4	Unspecified	Accuracy: 95.70% Precision: 91.90% Recall: 92.30% F1-score: 94.70%	Not used
Mggdadi et al. [53]	2021	TL	AD dataset kaggle	MRI	4	Unspecified	Accuracy: 70.30% Precision: — Recall:— F1-score: —	Not used
Murugan et al. [54]	2021	CNN	AD dataset kaggle	MRI	4	6,400 samples increased to 12,800 using the Synthetic Minority Over-sampling Technique (SMOTE)	Accuracy: 95.23% Precision: 96% Recall: 95% F1-score: 95.27%	Not used
Nicholas et al. [55]	2021	Combination of Local Binary Patterns (LBP) and KNN	AD dataset kaggle	MRI	4	6200	Accuracy: 91.21% Precision: — Recall:— F1-score: —	Not used
Kaplan et. al. [56]	2021	Local Phase Quantization Network (LPQNet)	AD dataset kaggle	MRI	2, 4	Unspecified	Accuracy:99.64, 99.62% Precision: 99.72, 99.74% Recall: —, 99.66% F1-score: 99.64, 99.70%	Not used
Sharma et al. [57]	2022	Hybrid AI-based model that combines both TL and permutation-based ML voting classifier	AD dataset kaggle	MRI	4	6126	Accuracy: 91.75% Precision: — Recall:— F1-score: 90.25%	Not used
Al-Adhaileh et al. [58]	2022	AlexNet	AD dataset kaggle	MRI	—	—	Accuracy: 94.53% Precision:— Recall:— F1-score: 94.12%	Not used
Ullah et al. [59]	2022	CNN	Alzheimer MRI preprocessed dataset kaggle	MRI	4	6,400 samples increased to 12,800 using SMOTE	Accuracy: 99.38% Precision: 99% Recall: 99% F1-score : 99%	Not used
Biswas et al. [60]	2022	CNN	AD dataset kaggle	MRI	2	4800	Accuracy: 99.38% Precision: 99.70% Recall: 95% F1-score: 99.32%	Not used
Proposed study	**2023**	**ViT-GRU**	**Alzheimer MRI preprocessed dataset kaggle**	**MRI**	**4**	**6400**	**Accuracy: 99.53% Precision: 99.53% Recall: 99.53% F1-score: 99.53%**	**Used**
				MRI	**2**	**6400**	**Accuracy: 99.69% Precision: 99.69% Recall: 99.69% F1-score: 99.69%**	
			ADNI	**MRI**	**3**	**2970**	**Accuracy: 99.26% Precision: 99.27% Recall: 99.26% F1-score: 99.26%**	

model aligns with their expertise and clinical knowledge. The inclusion of XAI techniques distinguishes our study from previous works and highlights its potential for practical implementation in healthcare settings.

Our analysis of the DL model's performance using LIME, SHAP, and Attention map has yielded consistent results, indicating that the model accurately captures the key characteristics of AD. These techniques have highlighted several well-established hallmarks of the disease, including hippocampal atrophy, enlarged ventricles, cortical atrophy, and white matter lesions [50]. Such findings indicate that the model is effectively learning from the data and capturing

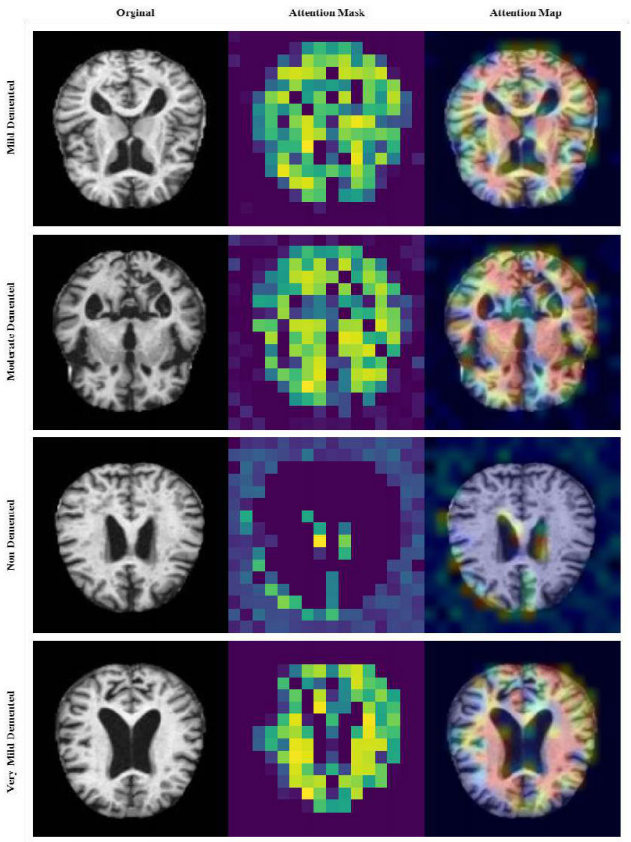

FIGURE 31. Attention map for dataset 1.

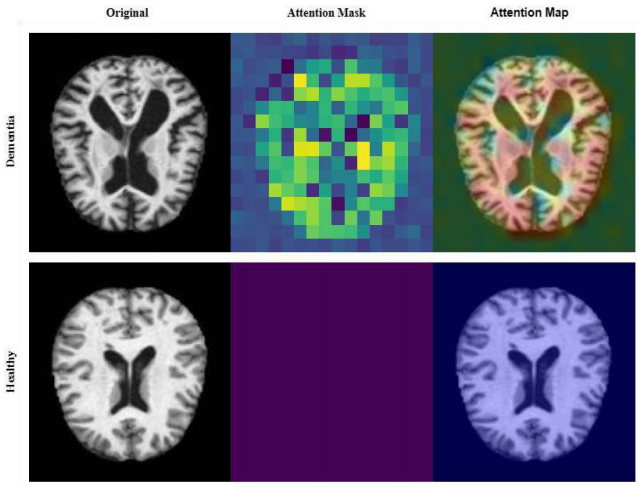

FIGURE 32. Attention map for dataset 2.

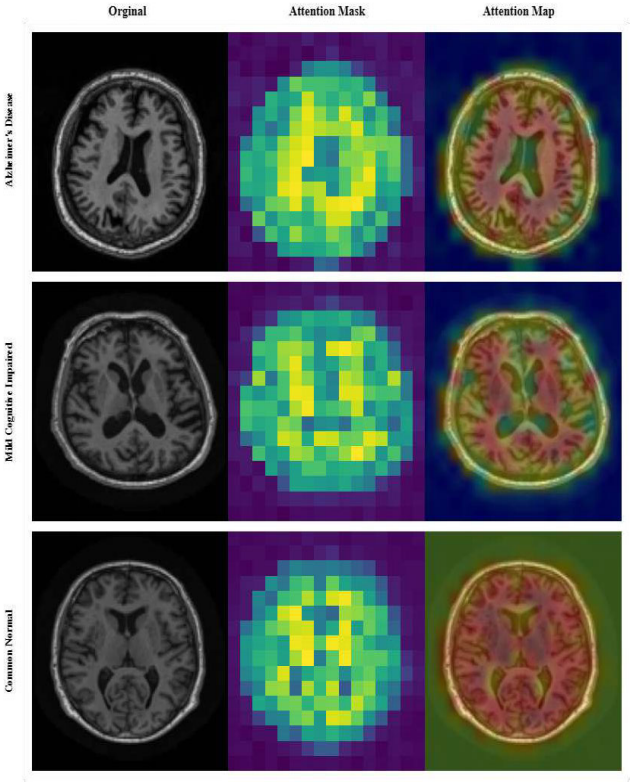

FIGURE 33. Attention map for dataset 3.

the underlying biology of AD. The insights gained from the LIME and SHAP analyses have significant implications for diagnosing and treating AD. By identifying the most critical features, clinicians can focus on these areas when interpreting MRI scans or other diagnostic tests. These can lead to earlier and more accurate diagnosis, which is critical for effective treatment and management of the disease.

We have presented our findings in Figures 25, 26, and 27 with each figure corresponding to a specific dataset (Dataset 1, Dataset 2, and Dataset 3) in the LIME analysis, accompanied by example images. Additionally, Figures 28, 29 and 30 depict results from the SHAP analysis, again corresponding to Dataset 1, Dataset 2, and Dataset 3 along with example images. Finally, Figures 31, 32, and 33 illustrate the outcomes of the Attention map analysis, once more linked to the respective datasets and featuring example images.

In addition, Table 9 comprehensively compares notable AD classification approaches, considering factors such as dataset, number of classes, classification method, image count, and performance metrics. It highlights the diversity in AD classification, with varying datasets and class distinctions. Different techniques, including traditional ML algorithms and DL models, are used for classification. The number of images varies, indicating dataset sizes. Performance metrics such as accuracy, precision, recall, F1-score, specificity, and Cohen's kappa value demonstrate the effectiveness of different approaches. The proposed ViT-GRU model outperforms other models and algorithms, showcasing its potential as a state-of-the-art approach in AD classification, leveraging self-attention and RNN.

A. FUTURE WORK

The model proposed in this study can be subjected to further evaluation on more extensive and diverse datasets to assess its effectiveness and generalizability in real-world scenarios.

Furthermore, the model can be extended to include other biomarkers, such as genetic markers and cerebrospinal fluid, to improve the accuracy of AD diagnosis.

VII. CONCLUSION

In conclusion, this study presents a novel approach for accurate AD classification using a ViT-GRU model and XAI techniques. The proposed model demonstrates superior performance on Dataset 1, Dataset 2, and Dataset 3, respectively. These results outperform that of existing methods and confirm the effectiveness of the ViT-GRU model in accurately identifying AD characteristics from MRI images. The incorporation of XAI techniques further enhances the model's interpretability, allowing clinicians to understand the decision-making process and gain insights into the factors driving AD diagnosis. By visualizing the significant features contributing to the model's predictions, clinicians can make informed decisions and improve clinical interventions. The ViT-GRU model also demonstrates superior performance compared to other pre-trained models, taking less time to train and providing the best accuracy, precision, recall, F1-score, specificity, and Cohen's kappa value. Overall, this study highlights the potential of the ViT-GRU model and XAI techniques in accurately classifying AD, providing valuable insights for clinicians, and opening avenues for real-world clinical applications. The proposed framework holds promise for early and accurate AD diagnosis, enabling timely interventions and improved patient care.

DATA AVAILABILITY

The data used to support the findings of this study are available from the corresponding author upon request.

AUTHOR CONTRIBUTION

S. M. Mahim: conceptualization, formal analysis, methodology, software, data curation, validation, writing—original draft, and review and editing; Md. Shahin Ali: methodology, software, validation, and writing—review and editing; Md. Olid Hasan: data curation, writing and validation; Abdullah Al Nomaan Nafi: data curation, writing, validation, and visualization; Arefin Sadat: data curation, writing, and validation; Shakib Al Hasan: data curation, writing, and validation; Bryar Shareef: methodology and writing—review and editing; Md. Manjurul Ahsan: investigation and writing—review and editing; Md. Khairul Islam: methodology, formal analysis, validation, writing—review and editing, and supervision; Md. Sipon Miah: writing—review and editing; and Ming-Bo Niu: writing—review and editing, and project administration.

COMPETING INTEREST

The authors declare that there is no conflict of interest regarding the publication of this article.

ACKNOWLEDGMENT

The authors would like to thank the support provided by the Bio-Imaging Research Laboratory, Department of Biomedical Engineering, Islamic University, Kushtia, Bangladesh, in carrying out their research successfully.

REFERENCES

[1] J. Weller and A. Budson, "Current understanding of Alzheimer's disease diagnosis and treatment," *F1000Res.*, vol. 7, p. 9, Jul. 2018.
[2] P. N. Tariot, "Alzheimer disease: An overview," *Alzheimer Disease Associated Disorders*, vol. 8, no. 2, p. S12, 1994.
[3] S. Liu, S. Liu, W. Cai, H. Che, S. Pujol, R. Kikinis, D. Feng, and M. J. Fulham, "Multimodal neuroimaging feature learning for multiclass diagnosis of Alzheimer's disease," *IEEE Trans. Biomed. Eng.*, vol. 62, no. 4, pp. 1132–1140, Apr. 2015.
[4] A. Association, "Alzheimer's disease facts and figures," *Alzheimer's Dementia*, vol. 15, pp. 321–387, Mar. 2019.
[5] R. Castellani, R. Rolston, and M. Smith, "Alzheimer disease," *Disease-a-Month, DM*, vol. 56, pp. 484–546, Sep. 2010.
[6] M. K. Islam, M. S. Ali, M. S. Miah, M. M. Rahman, M. S. Alam, and M. A. Hossain, "Brain tumor detection in MR image using superpixels, principal component analysis and template based K-means clustering algorithm," *Mach. Learn. Appl.*, vol. 5, Sep. 2021, Art. no. 100044.
[7] M. S. Alam, M. M. Rahman, M. A. Hossain, M. K. Islam, K. M. Ahmed, K. T. Ahmed, B. C. Singh, and M. S. Miah, "Automatic human brain tumor detection in MRI image using template-based K means and improved fuzzy C means clustering algorithm," *Big Data Cognit. Comput.*, vol. 3, no. 2, p. 27, May 2019.
[8] S. G. Mueller, M. W. Weiner, L. J. Thal, R. C. Petersen, C. R. Jack, W. Jagust, J. Q. Trojanowski, A. W. Toga, and L. Beckett, "Ways toward an early diagnosis in Alzheimer's disease: The Alzheimer's disease neuroimaging initiative (ADNI)," *Alzheimer's Dementia*, vol. 1, no. 1, pp. 55–66, Jul. 2005.
[9] C. Laske, H. R. Sohrabi, S. M. Frost, K. López-de-Ipiña, P. Garrard, M. Buscema, J. Dauwels, S. R. Soekadar, S. Mueller, C. Linnemann, S. A. Bridenbaugh, Y. Kanagasingam, R. N. Martins, and S. E. O'Bryant, "Innovative diagnostic tools for early detection of Alzheimer's disease," *Alzheimer's Dementia*, vol. 11, pp. 561–578, May 2015.
[10] C. Ieracitano, N. Mammone, A. Hussain, and F. C. Morabito, "A novel multi-modal machine learning based approach for automatic classification of EEG recordings in dementia," *Neural Netw.*, vol. 123, pp. 176–190, Mar. 2020.
[11] E. Moser, A. Stadlbauer, C. Windischberger, H. Quick, and M. E. Ladd, "Magnetic resonance imaging methodology," *Eur. J. Nuclear Med. Mol. Imag.*, vol. 36, pp. 30–41, Dec. 2008.
[12] L. J. Herrera, I. Rojas, H. Pomares, A. Guillén, O. Valenzuela, and O. Baños, "Classification of MRI images for Alzheimer's disease detection," in *Proc. Int. Conf. Social Comput.*, Sep. 2013, pp. 846–851.
[13] N. Yamanakkanavar, J. Y. Choi, and B. Lee, "MRI segmentation and classification of human brain using deep learning for diagnosis of Alzheimer's disease: A survey," *Sensors*, vol. 20, no. 11, p. 3243, Jun. 2020.
[14] S. Basheer, S. Bhatia, and S. B. Sakri, "Computational modeling of dementia prediction using deep neural network: Analysis on OASIS dataset," *IEEE Access*, vol. 9, pp. 42449–42462, 2021.
[15] S. Liu, S. Liu, W. Cai, S. Pujol, R. Kikinis, and D. Feng, "Early diagnosis of Alzheimer's disease with deep learning," in *Proc. IEEE 11th Int. Symp. Biomed. Imag. (ISBI)*, Apr. 2014, pp. 1015–1018.
[16] A. Ortiz, J. Munilla, J. M. Górriz, and J. Ramírez, "Ensembles of deep learning architectures for the early diagnosis of the Alzheimer's disease," *Int. J. Neural Syst.*, vol. 26, no. 7, Nov. 2016, Art. no. 1650025.
[17] R. Ju, C. Hu, P. Zhou, and Q. Li, "Early diagnosis of Alzheimer's disease based on resting-state brain networks and deep learning," *IEEE/ACM Trans. Comput. Biol. Bioinf.*, vol. 16, no. 1, pp. 244–257, Jan. 2019.
[18] H. Nawaz, M. Maqsood, S. Afzal, F. Aadil, I. Mehmood, and S. Rho, "A deep feature-based real-time system for Alzheimer disease stage detection," *Multimedia Tools Appl.*, vol. 80, nos. 28–29, pp. 35789–35807, Nov. 2021.
[19] S. Basaia, F. Agosta, L. Wagner, E. Canu, G. Magnani, R. Santangelo, and M. Filippi, "Automated classification of Alzheimer's disease and mild cognitive impairment using a single MRI and deep neural networks," *NeuroImage, Clin.*, vol. 21, Feb. 2019, Art. no. 101645.
[20] H. Sun, A. Wang, W. Wang, and C. Liu, "An improved deep residual network prediction model for the early diagnosis of Alzheimer's disease," *Sensors*, vol. 21, no. 12, p. 4182, Jun. 2021.

[21] R. Jain, N. Jain, A. Aggarwal, and D. J. Hemanth, "Convolutional neural network based Alzheimer's disease classification from magnetic resonance brain images," *Cognit. Syst. Res.*, vol. 57, pp. 147–159, Oct. 2019.
[22] T. M. Schouten, M. Koini, F. D. Vos, S. Seiler, M. D. Rooij, A. Lechner, R. Schmidt, M. V. D. Heuvel, J. V. D. Grond, and S. A. R. B. Rombouts, "Individual classification of Alzheimer's disease with diffusion magnetic resonance imaging," *NeuroImage*, vol. 152, pp. 476–481, May 2017.
[23] C. Ge, Q. Qu, I. Y. Gu, and A. S. Jakola, "Multiscale deep convolutional networks for characterization and detection of Alzheimer's disease using MR images," in *Proc. IEEE Int. Conf. Image Process. (ICIP)*, Sep. 2019, pp. 789–793.
[24] C. Feng, A. Elazab, P. Yang, T. Wang, F. Zhou, H. Hu, X. Xiao, and B. Lei, "Deep learning framework for Alzheimer's disease diagnosis via 3D-CNN and FSBi-LSTM," *IEEE Access*, vol. 7, pp. 63605–63618, 2019.
[25] H. Allioui, M. Sadgal, and A. Elfazziki, "Deep MRI segmentation: A convolutional method applied to Alzheimer disease detection," *Int. J. Adv. Comput. Sci. Appl.*, vol. 10, no. 11, p. 7, 2019.
[26] A. Balasundaram, S. Srinivasan, A. Prasad, J. Malik, and A. Kumar, "Hippocampus segmentation-based Alzheimer's disease diagnosis and classification of MRI images," *Arabian J. Sci. Eng.*, vol. 48, pp. 1–17, Jan. 2023.
[27] M. H. T. Najaran, "A genetic programming-based convolutional deep learning algorithm for identifying COVID-19 cases via X-ray images," *Artif. Intell. Med.*, vol. 142, Aug. 2023, Art. no. 102571.
[28] L. Wu, L. Huang, M. Li, Z. Xiong, D. Liu, Y. Liu, S. Liang, H. Liang, Z. Liu, X. Qian, J. Ren, and Y. Chen, "Differential diagnosis of secondary hypertension based on deep learning," *Artif. Intell. Med.*, vol. 141, Jul. 2023, Art. no. 102554.
[29] M. S. Ali, M. S. Miah, J. Haque, M. M. Rahman, and M. K. Islam, "An enhanced technique of skin cancer classification using deep convolutional neural network with transfer learning models," *Mach. Learn. Appl.*, vol. 5, Sep. 2021, Art. no. 100036.
[30] M. K. Islam, M. M. Rahman, M. S. Ali, S. M. Mahim, and M. S. Miah, "Enhancing lung abnormalities detection and classification using a deep convolutional neural network and GRU with explainable AI: A promising approach for accurate diagnosis," *Mach. Learn. Appl.*, vol. 14, Dec. 2023, Art. no. 100492.
[31] M. S. Ali, M. K. Islam, A. A. Das, D. U. S. Duranta, M. F. Haque, and M. H. Rahman, "A novel approach for best parameters selection and feature engineering to analyze and detect diabetes: Machine learning insights," *BioMed Res. Int.*, vol. 2023, pp. 1–15, May 2023.
[32] D. U. S. Duranta, M. S. Ali, A. A. Das, M. M. Rahman, M. M. Ahsan, M. S. Miah, and M. K. Islam, "Enhancing atrial fibrillation detection accuracy: A wavelet transform filtered single lead ECG signal analysis with artificial neural networks and novel feature extraction," *Mach. Learn. Appl.*, vol. 12, Jun. 2023, Art. no. 100472.
[33] M. K. Islam, M. S. Ali, M. M. Ali, M. F. Haque, A. A. Das, M. M. Hossain, D. S. Duranta, and M. A. Rahman, "Melanoma skin lesions classification using deep convolutional neural network with transfer learning," in *Proc. 1st Int. Conf. Artif. Intell. Data Analytics (CAIDA)*, Apr. 2021, pp. 48–53.
[34] S. Picciolini, A. Gualerzi, C. Carlomagno, M. Cabinio, S. Sorrentino, F. Baglio, and M. Bedoni, "An SPRi-based biosensor pilot study: Analysis of multiple circulating extracellular vesicles and hippocampal volume in Alzheimer's disease," *J. Pharmaceutical Biomed. Anal.*, vol. 192, Jan. 2021, Art. no. 113649.
[35] M. M. Hossain, M. S. Ali, M. M. Ahmed, M. R. H. Rakib, M. A. Kona, S. Afrin, M. K. Islam, M. M. Ahsan, S. M. R. H. Raj, and M. H. Rahman, "Cardiovascular disease identification using a hybrid CNN-LSTM model with explainable AI," *Informat. Med. Unlocked*, vol. 42, Oct. 2023, Art. no. 101370.
[36] W. Seeley, "Frontotemporal dementia neuroimaging: A guide for clinicians," *Dementia Clin. Pract.*, vol. 24, pp. 160–167, Jan. 2009.
[37] A. A. Lima, M. F. Mridha, S. C. Das, M. M. Kabir, M. R. Islam, and Y. Watanobe, "A comprehensive survey on the detection, classification, and challenges of neurological disorders," *Biology*, vol. 11, no. 3, p. 469, Mar. 2022.
[38] J. Smucny, G. Shi, and I. Davidson, "Deep learning in neuroimaging: Overcoming challenges with emerging approaches," *Frontiers Psychiatry*, vol. 13, p. 7, Jun. 2022.
[39] K. Rasheed, A. Qayyum, M. Ghaly, A. Al-Fuqaha, A. Razi, and J. Qadir, "Explainable, trustworthy, and ethical machine learning for healthcare: A survey," *Comput. Biol. Med.*, vol. 149, Oct. 2022, Art. no. 106043.
[40] N. Naik, B. M. Z. Hameed, D. K. Shetty, D. Swain, M. Shah, R. Paul, K. Aggarwal, S. Ibrahim, V. Patil, K. Smriti, S. Shetty, B. P. Rai, P. Chlosta, and B. K. Somani, "Legal and ethical consideration in artificial intelligence in healthcare: Who takes responsibility?" *Frontiers Surgery*, vol. 9, p. 266, Mar. 2022.
[41] S. Kumar. (2021). *Alzheimer MRI Dataset*. Accessed: May 3, 2023. [Online]. Available: https://www.kaggle.com/datasets/sachinkumar413/alzheimer-mri-dataset
[42] Initiative. (2023). *Alzheimer's Disease*. [Online]. Available: https://adni.loni.usc.edu/
[43] N. Sheikh-Bahaei, S. A. Sajjadi, R. Manavaki, and J. H. Gillard, "Imaging biomarkers in Alzheimer's disease: A practical guide for clinicians," *J. Alzheimer's Disease Rep.*, vol. 1, no. 1, pp. 71–88, Jul. 2017.
[44] R. Mohtasib, J. Alghamdi, A. Jobeir, A. Masawi, N. P. de Barros, T. Billiet, H. Struyfs, T. V. Phan, W. Van Hecke, and A. Ribbens, "MRI biomarkers for Alzheimer's disease: The impact of functional connectivity in the default mode network and structural connectivity between lobes on diagnostic accuracy," *Heliyon*, vol. 8, no. 2, Feb. 2022, Art. no. e08901.
[45] M. I. Hasan, M. S. Ali, M. H. Rahman, and M. K. Islam, "Automated detection and characterization of colon cancer with deep convolutional neural networks," *J. Healthcare Eng.*, vol. 2022, pp. 1–12, Aug. 2022.
[46] A. Vaswani, N. Shazeer, N. Parmar, J. Uszkoreit, L. Jones, A. Gomez, Ł. Kaiser, and I. Polosukhin, "Attention is all you need," in *Proc. Adv. Neural Inf. Process. Syst.*, vol. 30, 2017, pp. 1–11.
[47] J. Chung, C. Gulcehre, K. Cho, and Y. Bengio, "Empirical evaluation of gated recurrent neural networks on sequence modeling," 2014, *arXiv:1412.3555*.
[48] M. Ribeiro, S. Singh, and C. Guestrin, "'Why should I trust you?' Explaining the predictions of any classifier," in *Proc. 22nd ACM SIGKDD Int. Conf. Knowl. Discovery Data Mining*, 2016, pp. 1135–1144.
[49] S. Lundberg and S. Lee, "A unified approach to interpreting model predictions," in *Proc. Adv. Neural Inf. Process. Syst.*, vol. 30, 2017, pp. 1–10.
[50] C. R. Jack, D. A. Bennett, K. Blennow, M. Carrillo, B. Dunn, S. Haeberlein, D. Holtzman, W. Jagust, F. Jessen, J. Karlawish, E. Liu, J. L. Molinuevo, T. Montine, C. Phelps, K. P. Rankin, C. C. Rowe, P. Scheltens, E. Siemers, H. M. Heather, and R. Sperling, "NIA-AA research framework: Toward a biological definition of Alzheimer's disease," *Alzheimer's Dementia*, vol. 14, no. 4, pp. 535–562, Apr. 2018.
[51] H. Wang, Y. Shen, S. Wang, T. Xiao, L. Deng, X. Wang, and X. Zhao, "Ensemble of 3D densely connected convolutional network for diagnosis of mild cognitive impairment and Alzheimer's disease," *Neurocomputing*, vol. 333, pp. 145–156, Mar. 2019.
[52] H. Acharya, R. Mehta, and D. K. Singh, "Alzheimer disease classification using transfer learning," in *Proc. 5th Int. Conf. Comput. Methodologies Commun. (ICCMC)*, Apr. 2021, pp. 1503–1508.
[53] E. Mggdadi, A. Al-Aiad, M. S. Al-Ayyad, and A. Darabseh, "Prediction Alzheimer's disease from MRI images using deep learning," in *Proc. 12th Int. Conf. Inf. Commun. Syst. (ICICS)*, May 2021, pp. 120–125.
[54] S. Murugan, C. Venkatesan, M. G. Sumithra, X.-Z. Gao, B. Elakkiya, M. Akila, and S. Manoharan, "DEMNET: A deep learning model for early diagnosis of Alzheimer diseases and dementia from MR images," *IEEE Access*, vol. 9, pp. 90319–90329, 2021.
[55] B. Nicholas, A. Jayakumar, B. Titus, and T. R. Nair, "Comparative study of multiple feature descriptors for detecting the presence of Alzheimer's disease," *Ubiquitous Intell. Syst.*, vol. 243, pp. 331–339, Oct. 2022.
[56] E. Kaplan, S. Dogan, T. Tuncer, M. Baygin, and E. Altunisik, "Feed-forward LPQNet based automatic Alzheimer's disease detection model," *Comput. Biol. Med.*, vol. 137, Oct. 2021, Art. no. 104828.
[57] S. Sharma, S. Gupta, D. Gupta, A. Altameem, A. K. J. Saudagar, R. C. Poonia, and S. R. Nayak, "HTLML: Hybrid AI based model for detection of Alzheimer's disease," *Diagnostics*, vol. 12, no. 8, p. 1833, Jul. 2022.
[58] M. H. Al-Adhaileh, "Diagnosis and classification of Alzheimer's disease by using a convolution neural network algorithm," *Soft Comput.*, vol. 26, no. 16, pp. 7751–7762, Aug. 2022.
[59] Z. Ullah and M. Jamjoom, "A deep learning for Alzheimer's stages detection using brain images," *Comput., Mater. Continua*, vol. 74, no. 1, pp. 1457–1473, 2023.
[60] M. Biswas, M. Mahbub, and M. Miah, "An enhanced deep convolution neural network model to diagnose Alzheimer's disease using brain magnetic resonance imaging," in *Proc. 4th Int. Conf. Recent Trends Image Process. Pattern Recognit.*, Msida, Malta, May 2022, pp. 42–52.

S. M. MAHIM is currently pursuing the bachelor's degree in biomedical engineering with Islamic University, Kushtia. His research interests include the intersection of healthcare and technology, with a focus on machine learning and deep learning, with a passion for computer vision, medical image processing, medical signal processing, and medical data analysis. He has consistently demonstrated a commitment to academic excellence. He has engaged in several research projects, showcasing their strong analytical skills and collaborative ability. With a commitment to staying up-to-date with the latest developments in the field, he is poised to make a meaningful contribution to the future of healthcare through technology.

MD. SHAHIN ALI received the B.Sc. (Engg.) degree from the Department of Biomedical Engineering. He is currently pursuing the M.Sc. degree with the Department of Biomedical Engineering, Islamic University, Kushtia, Bangladesh. He has been a Research Assistant with the Bio-Imaging Research Laboratory, since June 2020. His exceptional academic performance has earned him recognition and respect among his peers and professors. His research interests include medical image processing, signal processing, computer vision, machine learning, deep learning, cognitive radio networks, and health informatics, reflecting his commitment to advancing the field of biomedical engineering. His dedication and passion for the discipline have led him to enroll in the master's program with the Department of Biomedical Engineering, with the aim of expanding his knowledge and expertise further. As a recognized reviewer for reputable journals, his contributions to the same field are noteworthy. With his exceptional academic achievements, research contributions, and enthusiasm, he is poised to make significant contributions to the field of biomedical engineering.

MD. OLID HASAN is currently pursuing the B.Sc. degree in biomedical engineering with Islamic University, Bangladesh. He passed with good academic results in higher secondary school certificates. His research interests include advancements in medical imaging, medical data analysis, experimental design, the intersection of engineering, and healthcare. He is dedicated to leveraging their educational pursuits to contribute to advancements in biomedical engineering (BME).

ABDULLAH AL NOMAAN NAFI is currently pursuing the bachelor's degree in information and communication technology. He possesses a strong fascination for the intersection of healthcare and technology. His academic focus centers on machine learning, deep learning, and natural language processing, with a distinct inclination towards computer vision, medical image processing, signal processing, medical image captioning, and medical data analysis. Throughout his academic journey, he has consistently showcased his dedication to achieving excellence in his studies. He has actively participated in numerous research projects, underscoring his adeptness in analytical thinking and collaborative teamwork. With an unwavering commitment to staying abreast of the latest advancements in the field, he is poised to make a substantial and impact contribution to the realms of healthcare and computer vision through the power of technology.

AREFIN SADAT is a final-year MBBS student of Chandpur Medical College, Bangladesh. He has been selected and pursuing his research elective with the Kamineni Institute of Medical Science (KIMS), India, under the supervision of Prominent Indian Clinical Researcher and Medicine Specialist Dr. Rakesh Biswas. Furthermore, he writes columns in the leading English newspapers. Moreover, he was actively involved in Notre Dame Debating Club. He is also the President of the Chandpur Medical College Debating Club. He was also the Winning Team Leader of the Inter-Medical Debate Competition organized by the Platform of Doctors and Medical Students Society, in 2021. At this edge, he is looking forward to incorporating his leadership and research experiences and skills to mitigate the drastic health service issues through various research projects. He has got GPA 5 in all of his board examinations and availed the national scholarship and stood 27th merit position in Savar Upazilla under Dhaka Board in the SSC examination.

SHAKIB AL HASAN is currently pursuing the B.Sc. degree with the Department of Biomedical Engineering (BME), Islamic University, Kushtia, Bangladesh. He is also a Research Assistant in AI and computer vision with the Image Processing Laboratory, Department of Biomedical Engineering, Islamic University. He successfully completed a well-organized higher secondary and a secondary school certificate in the science discipline with good outcomes. Moreover, he is passionate about medical AI, including medical image processing, health informatics, natural language processing, machine learning, and deep learning.

BRYAR SHAREEF received the Ph.D. degree in computer science from the University of Idaho, Idaho Falls, USA, in 2023. He is currently an Assistant Professor with the University of Nevada, Las Vegas. His scholarly pursuits center around biomedical image analysis, computer vision, deep learning, machine learning, and health informatics. His research interests include the application of these disciplines in critical domains, notably in the realm of medical imaging, and diagnosis.

MD. MANJURUL AHSAN received the M.S. degree in industrial engineering from Lamar University, USA, in 2018, and the Ph.D. degree in industrial and systems engineering from The University of Oklahoma, Norman, USA, in 2023. He is currently a Research Scholar with the Machine and Hybrid Intelligence Laboratory, School of Medicine, Northwestern University. His research interests include image processing, computer vision, deep learning, machine learning, and model optimization as applied to high-risk applications, such as medical imaging and diagnosis.

MD. KHAIRUL ISLAM received the M.Sc. degree in information and communication technology (ICT) from the Department of ICT Bangladesh, Islamic University, Kushtia, Bangladesh, in 2011, where he is currently pursuing the Ph.D. degree with the Department of Biomedical Engineering (BME). He is also an Assistant Professor with BME, Islamic University. He was a former Lecturer with the Department of Computer Science and Engineering (CSE), Prime University, Dhaka. Besides teaching, he was a Researcher and a former Researcher under the Ministry of Information and Communication Technology Division, Bangladesh, from 2013 to 2015. His research interests include medical image processing, machine learning, deep learning, the Internet of Things, and health informatics.

MD. SIPON MIAH (Senior Member, IEEE) was born in Gaibandha, Bangladesh, in January 1982. He received the B.Sc., M.Sc., and Ph.D. degrees from the Department of Information and Communication Technology (ICT), Islamic University, Kushtia, Bangladesh, in 2006, 2007, and 2016, respectively, and the Ph.D. degree in computer science from the University of Galway, Galway, Ireland, in June 2021. Since 2010, he has been with the Department of Information and Communication Technology, Islamic University, where he is currently a Professor with the Department of ICT. He is also a Postdoctoral Fellow with the Department of Signal Theory and Communications, University Carlos III of Madrid (UC3M), Leganes, Madrid, Spain. He was a recipient of the three years research grant funded by UC3M under the prestigious ''30 Postdoctoral Fellowship,'' in October 2021, and the four years structured Ph.D. ''Hardiman Scholarship'' funded by the University of Galway, in September 2016. His research interests include the cognitive radio-based Internet of Things, machine learning/deep learning-based wireless communications, THz communications, optimization-based wireless communications, and massive MIMO antennas-based wireless communications. The above research lines have produced more than 60 publications on international journals, presentations within international conferences, and book chapters with a total number of the citations more than 855 and H-index of 13 reported by Google Scholar. He also acts as a referee in several highly reputed journals and international conferences.

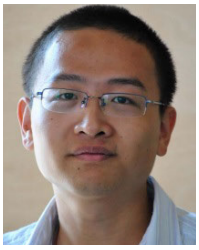

MING-BO NIU (Member, IEEE) received the B.Eng. degree in electronic engineering and the M.Sc. (Eng.) (Hons.) degree in communication and information systems from Northwestern Polytechnical University, China, and the Ph.D. degree in electrical and computer engineering from The University of British Columbia, Canada. Prior to the Ph.D. degree, he was with the State Key Laboratory on Underwater Information and Signal Processing. From 2008 to 2012, he was a Research Assistant with the Optical Wireless Communications Laboratory and the Integrated Optics Laboratory, where he contributed to the development of ultra-high speed optical data transmission links. He held a postdoctoral fellowship with Queen's University, Canada, for two years. He was also with Public Works at Calian Tech Ltd., where he contributed to highly efficient statistical evaluation models of MIMO compressive sensing projects. He is currently the Director of the Provincial International Innovation Research Centre, and heading the IVR Low Carbon Research Institute, Chang'an University, Shaanxi, China. He has served as a General Chair of the 3rd International Conference on Intelligent Traffic Systems and Smart City (ITSSC), Xi'an, China, in November 2023. He has coauthored more than 30 Institute of Electrical and Electronics Engineers (IEEE) and Optical Society of America (OSA) papers and supervised numerous projects. He also serves as an Academic Editor for *IntechOpen*. He is a member of the Internet of Things (IoT) Committee at the China Institute of Communications (CIC). He received numerous scholarships during his undergraduate and graduate studies, including the Chinese Government Award, two The University of British Columbia University Graduate Fellowships (UGFs), and a Huawei Tech Ltd., Special Fellowship. His current research interests include the Internet of Vehicles (IoV), vehicle-to-road (V2R) infrastructure, cooperative microgrids, massive multiple input, multiple outputs (MIMO), image signal processing, low-carbon smart cities, energy harvesting, and electronic circuit theory. He is a Licensed Professional Engineer in British Columbia.